ß-PHENYLETHYLAMINE: A NOVEL CHEMO-ATTRACTANT AGENT

A Thesis
Submitted to the Graduate Faculty
of the
North Dakota State University
of Agriculture and Applied Science

By

August Henry Burg

In Partial Fulfillment of the Requirements
for the Degree of
MASTER OF SCIENCE

Major Program:
Microbiology

April 2020

Fargo, North Dakota

North Dakota State University
Graduate School

Title

ß-Phenylthylamine: A Novel Chemo-attractant Agent

By

August Henry Burg

The Supervisory Committee certifies that this ***disquisition*** complies with North Dakota State University's regulations and meets the accepted standards for the degree of

MASTER OF SCIENCE

SUPERVISORY COMMITTEE:

Birgit Pruess
Chair

Jane Schuh

Glenn Dorsam

Mark McCourt

Approved:

April 15th, 2021
Date

John McEvoy
Department Chair

ABSTRACT

Bacterial metabolism and physiology are finely tuned mechanisms that maintain homeostasis for the bacterium and allow for responses to environmental signals. Responses could include anything from regulation of cell division to the expression of virulence factors leading to serious infection. This thesis explores the role of neurotransmitter molecules and ß-phenylethylamine (a structurally similar molecule to catecholamines) on the physiological characteristics of *flhD* expression, biofilm formation, and chemotactic behaviors in the *E. coli* organism. We observed changes in physiology leading to chemotactic changes in the presence of ß-phenylethylamine through the Plug Agarose Assay as well as the Microfluidic Assay. In a comparison with serine, the amino acid and documented chemoattractant agent, ß-phenylethylamine was revealed to be a novel chemoattractant agent with comparable influence on the bacterium.

ACKNOWLEDGMENTS

I extend my gratitude to my friends and colleagues, the faculty and staff of the Department of Microbiological Sciences at North Dakota State University. In particular, Shelley Horne is greatly deserving of thanks for her assistance in procuring reagents as well as advising in the technical aspect of the experiments performed in Van Es.

I also wish to acknowledge our partnership with colleagues at The Agricultural and Mechanical College of Texas, specifically the laboratory of Arul Jayaraman, the technical knowledge of Nitesh Sule, and the expertise of Michael Manson were integral in the development of this project. Their input has made an immense positive impact on this study.

Lastly, I wish to acknowledge Dr. Birgit Pruess, my research mentor and advisor through this project. With her, the questions and methods were developed to expand the realm of experimentation seen by her laboratory which are now of interest to current students. Thank you for your help and support!

TABLE OF CONTENTS

LIST OF TABLES

LIST OF FIGURES

INTRODUCTION

Microorganisms, including pathogens, can be found ubiquitously through biotic environments and have even been traced to places devoid of larger eukaryotic lifeforms (Ramette et al., 2007). As such, these organisms can be found on the surfaces of crops, in livestock, and can be transmitted into human environments (Horner-Devine et al., 2004). Though much of the bacterial and fungal flora found in humans exists in a commensal fashion, pathogenic organisms introduced from the environment may lead to disruptions in normal metabolism and activity of both the host and endogenous microbial species (Pankey et al., 2017). One specific concern of infectious disease includes infection due to ingesting contaminated food, resulting in a broad class of diseases known to national agencies as foodborne illness. Of these, *E. coli* O157:H7 is of particular concern, with three outbreaks in November and December of 2019 (CDC: *E. coli*, 2019).

With 48 million Americans becoming infected by foodborne illnesses per annum, impacts on economic measures are substantial (Hoffmann et al., 2015). Nearly 3,000 deaths per year in the USA are attributed to foodborne disease and related complications, while nearly $15.5 billion in economic burdens are calculated by federal agencies (CDC, 2019). Incidence of foodborne disease has become a great healthcare fear, with large scale food production leading to wide-spread outbreaks. Pathogenic *E. coli* strains alone have represented well over 25 wide-spread outbreaks since 2005, placing extra strain on healthcare systems (CDC: *E. coli*, 2019).

Biofilm forming bacteria also present challenges for sterilization on medical equipment and food preparation surfaces (Lindsay et al., 2002). The ability of organisms to adhere to and disperse from biofilms is a contributing factor to the infection of implanted materials and intravenous catheters, both of which lead to disease related to medical care (Costerton et al.,

1995). Methods of microbial control select for resistant strains and increase the urgency for the development of novel anti-microbial therapies and treatments (Kirby, 1944).

In the case of pathogenic *E. coli* O157:H7 (Enterohemorrhagic *E. coli,* or EHEC), a normal organism found in the intestinal tracts of ruminant organisms, agricultural and food preparation methods have led to accidental contamination of food and food products for human consumption often on an international scale (Zhao et al., 1995). The resulting illness of *E. coli* infection is caused by the metabolic activity of the bacterium in the host's intestinal tract, where the bacterium is exposed to molecules both derived from the host's diet and molecules secreted directly by the host (Croxen et al., 2013).

One mechanism for the pathogenesis of EHEC is activated inside the human host by molecules such as epinephrine and norepinephrine, which are secreted into the lumen of the intestine by leaky tissues in Peyer's Patches (Hughes et Sperandio, 2008). The bacterium first finds its way to the intestine by ingestion and regular gut peristalsis, and then deposes itself and initiates a transition to a sessile life in a bacterial biofilm. From here, the bacterium causes damage to the host epithelium through Type III secretion systems (Cameron et al., 2015). The pathogenesis of EHEC results in structural damage to the epithelial cells of the intestine, which in turn leads to bloody diarrhea, intestinal cramping, and in extreme cases, may lead to death (Kaper et al., 2004).

Bacterial biofilms indicate populations of bacteria which cement themselves to a surface in an extracellular polymeric matrix, including biotic surfaces such as the intestinal wall or abiotic surfaces like stainless steel or plastics (Van Houdt et al., 2005). As *E. coli* bacteria congregate on the surface of the intestine, they attach using mucus-like molecules in which the

bacteria will continue to grow and be released. From here, spread of the bacteria from a central reservoir is possible.

As a common model organism which has a well-studied genetic and physiological background, as well as a pathogen in certain strains, *E. coli* lends itself well to use in microbiological studies. Most known *E. coli* strains are non-pathogenic (CDC: *E. coli*, 2019), but with many similar physiological characteristics that would feed into pathogenesis of pathogenic strains, responses of the pathogenic strains may be inferred.

The means by which *E. coli* moves through liquid and semi-solid media is flagellar motility and chemotaxis. The means by which *E. coli* remain sessile on surfaces and on liquid-air interfaces is its ability to form biofilms. In addition, the potential for some molecules, such as human derived compounds, to stimulate changes in the bacteria's physiology related to both chemotactic activity as well as the activation of signaling pathways. These compounds can work to attract bacteria away from some regular type of flow, such as periodic peristalsis as well as activate pathogenic pathways when specifically inside of a mammalian host. In the intestines, this may have a direct influence on the deposition of the bacteria to their sessile lifestyles in a biofilm or to encourage unbiased motility. Further information about the regulation of these responses to the bacterium's surroundings may reveal places where scientific understanding is thin and current understanding of molecular biology may be furthered.

FlhD

For the bacterial motility to be possible, a network of genes must be expressed and protein structures assembled. These molecular structures are produced by the functioning of *flhDC.* The flagellar master operon *flhDC* consists of two genes: *flhD* and *flhC* (Bartlett et al., 1988). The transcription of FlhD/FlhC results in the formation of a complex which binds to the

upstream sequence of many genes, including *fliA* (Liu et al., 1994). Transcriptional regulation of *flhDC* is tied strongly to the metabolic systems in *E. coli* such as in carbon and nitrogen metabolism (Prüß et al. 2001). Insertions into the regulatory regions of *flhDC* leading to increases in transcription were noted for major increases in motility (Barker et al., 2004). The spontaneous insertions of small genetic elements into these regions also led to reductions and increases in *flhDC* (Horne et al., 2016).

The control for flagellar expression is directly impacted by the activities of several transcriptional regulators, many of which rely upon the transfer of phosphates by means of two component signaling systems (Igo et al., 1989). In the bacterium, the two-component signaling systems function as environmental sensors which lead to responses to external stimuli by the bacterium to maintain efficient homeostasis through tightly regulated gene expression. These systems are analogous in many ways to eukaryotic sensory apparatus, but instead of reliance upon stimuli of particular cell groups in organ systems or specific G-protein systems in a tissue, bacteria must rely upon all of these environmental stimuli as a single cell organism. In the example of osmolarity, *E. coli* response to changes in environmental solutes relies upon the EnvZ/OmpR system, which utilizes EnvZ autophosphorylation and a transfer of the phosphate to OmpR (Forst et al., 1989). The resultant outcome of this signaling produces many effects, such as alteration of the ratio of OmpF to OmpC porins when external osmolarity changes through *envZ* and *ompR* (Aiba et al., 1989).

The QseC/QseB (quorum sensing) system is integral in the regulation of the pathogenic nature of *E. coli* serotypes through activation of virulence genes (Hughes and Sperandio, 2008). QseCB is also interesting for its presence in strains inclined towards biofilm formation and its absence in the genome of those consistently planktonic bacterial species in proteobacteria

(Sperandio et al., 2002). Though the QseCB system functions within the regular parameters of signaling kinases which lead to a downstream expression cascade, they are interesting further due to the molecules to which they bind: α and ß adrenergic molecules, such as human catecholamines epinephrine and norepinephrine in addition to the autoinducer molecules useful for quorum sensing (Sperandio et al., 2003). Questions regarding the ability of bacteria to establish a firm quorum for the initiation of pathogenesis led in part to the discovery that, in the presence of the adrenergic compounds of the human nervous systems, QseCB was stimulated and led to activation of the LEE pathogenicity island similarly to stimulation by AI-2 (autoinducer-2) and AI-3 (Sperandio et al., 2003). QseCB is studied for its positive regulation of the LEE pathogenicity islands, specifically the type III secretion systems that lead to enterocyte effacement (Sperandio et al., 2001). In addition, QseCB is also implicated as a positive regulator of the genes *tynA* and *feaB,* which are implicated with the metabolic ties to bacterial chemotaxis in *E. coli* (Zeng et al, 2013).

As the QseCB system was originally named, quorum signaling between bacteria can be achieved through the autoinducer molecules synthesized by the expression of various *lux* genes in *E. coli* and other species (Surette et al., 1999). It is also apparent that the quorum signaling is not only between bacterial species who express such bacterial genes, but also between the bacteria and the mammalian host, whose neurotransmitter molecules may also stimulate the QseCB system. These are the ‘human derived compounds” to which bacteria respond, noted by research performed by David Hughes, which led to pathogenesis in the mammalian gut (Clarke et al, 2006).

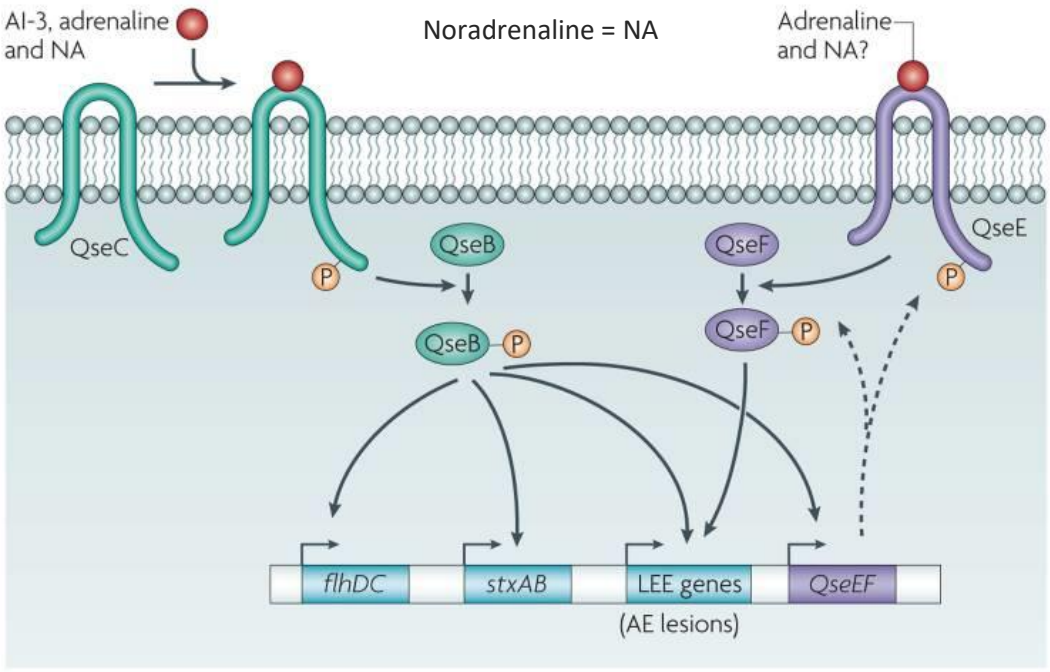

Figure 1*:* A Proposed Model for the Cascade of QseCB. Here, NA stands for noradrenaline. AI-3, adrenaline, and NA bind to QseC, which triggers autophosphorylation in the cytoplasm. From here, QseB is phosphorylated and acts to modulate transcription of *flhDC, stxAB,* and the LEE genes. Expression of the LEE genes is also modulated by the two-signal system *QseEF* (Hughes and Sperandio, 2008)

With two regulating systems are found upstream of the FlhDC transcriptional network and are partly responsible for the activity that leads to the synthesis, assembly, and utilization of flagella in *E. coli*. Additional downstream regulation of flagellar assembly and utilization, such as the activity of the sigma factor FliA, is integral to generate phenotypes of motility and chemotaxis (Fitzgerald et al., 2018). Specific for flagellar motility and chemotaxis, FliA fills many roles in several proteobacteria species and is also strongly conserved across many gram-positive species (Chen et al., 1992). From FliA, many genes specific to the physical apparatus of the flagellum are transcribed and assembled to create the flagellar motor complex.

The Flagellum and Taxis

The construction of the physical flagellum apparatus is the result of the *fliA* regulon, along with various other *flhDC* associated structural genes, and has been described as the product of stimulation of *flhDC* by several regulating two-component signaling systems (Kutsukake, 1994). The flagellum includes a Type III secretion system, which allows for protein units to be transported through the double membrane system (Wang et al., 2003). The flagellum FliC components are exported by the Type III secretion system and assemble at the tip of the growing structure to form the long organelle structure (Macnab, 2003). At the base of this structure sits a large reversible rotary motor powered by ion flux (Berg, 2003), which rotates the flagella. Regulation of the flagellar synthesis is not similarly driven by purely genetic regulation but as a process of phosphorylation events by a two-component system called CheAY (Sowa et al., 2008).

Permeating the membranes of *E. coli* are chemoreceptors that form a hexagonal lattice (Briegel et al., 2012). The classes of these methyl-accepting chemoreceptor proteins (MCPs) come in five known groups (Tsr, Tar, Trg, Tap, and Aer) and function in the environmental sensory activity for *E. coli* (Milligan et al., 1988). These MCPs are structurally conserved among bacteria, with species variation in the number encoded in the genome. Some species encode several dozen MCPs, such as *Pseudomonas* species (Szurmant et al., 2004). Activity triggered by binding of ligands leads to cytoplasmic interactions which influence the direct physiology of the bacterium (Falke et al., 2001). The MCP allows for external stimulation to cross the plasma by means of signaling systems, such as through the autophosphorylation of CheA.

Upon an MCP binding with a chemoattractant, a conformational change in CheW/A dimer complex leads to a halt to the autophosphorylation of the CheA protein which resides in

the cytoplasm (Roggo et al., 2019). CheA, functioning as a kinase, typically phosphorylates CheY, a constitutively expressed cytoplasmic protein in the absence of the chemoattractant (Surette et al., 1996). Under these circumstances with no chemoattractant , CheW associates with CheA, leading to the autophosphorylation of the latter. With CheA to phosphorylate CheY, the now prevalent CheY-P binds to FliM, and this leads to the charged residues changing conformation and holds the clockwise (CW) rotation orientation bias in the flagellar motor (Bren et al., 1998). Under high levels of external positive stimulation, CheA is separated from CheW, and no autophosphorylation occurs. CheZ, as protein with kinase activity, will dephosphorylate CheY-P as it makes its way to bind FliM. CheY-P in low concentration can be dephosphorylated before it binds the flagellar motor, and without being bound, FliM perpetuates the bacterium's default CCW swimming (Parkinson et al., 1979). The uncharged residues are most responsible for the default counter-clockwise CCW orientation, leading towards a flagellum bundle bias, but their influence in the activity of charged, clockwise motion is not definitive (Zhou et al., 1998). When chemoattractant stimulation ceases, CheAW association may be held momentarily by methylation of the dimer by CheR, which may be counteracted by the activity of CheB methylase (Berry et al., 1999).

E. coli may show a "chemotactic memory" by the methylation of the MCR bundle on the chemoreceptor for chemoattractants, leading to several seconds of "locked" formation and continual CheAY phosphorylation events conserving a CW rotation (Aizawa et al., 2000). The binding of the chemoattractant influences the bacterium's motility in its immediate environment from tumbling to smooth swimming. In a phenomenon known as run-and-tumble, periods of CW stagnation (tumbling) are intermittently interrupted by periods of smooth swimming CCW even with little or no external stimulation (Berg et Brown, 1972).

The activity of switching between the CCW and CW flagellar rotation bias is an interesting system rooted directly in the external signals: bacteria *without* external attracting stimulation rotate flagella in CW and are tumbling without specific direction, yet the *binding* of an attractant causes the flagella to switch to CCW rotation, which means the bacterium will be propelled and instead a straight-swimming period. Interestingly, as *E. coli* produce flagella throughout the cell in a peritrichous arrangement, the bacterium may sense changes in chemoattractant across the surface and length of the cell, with relatively high concentrations of CheY-P in one side of the bacterial rod leading to reductions in flagellar bundling and smooth swimming. This hypothesis would give further credence to the efficiency of the cell's ability to orient itself towards nutrient sources (Barnich et al., 2007).

TSR and Known E. coli Chemotactic Activity

The chemotactic signaling system in *E. coli* relies on the activity of just a few components which in turn rely on the aforementioned MCPs (Bouret et al., 2002). The *E. coli* chemotaxis proteins tend to cluster around one another in the membrane, and this clustering may be the basis for the overall sensitivity of the system (Kentner et Sourjik, 2006). It is estimated that the *E. coli* signaling pathway can amplify the stimulation signal and cause near 50% increased rotational bias (Segall et al., 1986). The chemoreceptor Tsr binds serine and tyrosine, Tar senses aspartate and maltose, Trg senses galactose and ribose, and Tap senses pyrimidines and dipeptides (Karavolos et al., 2013). Upon binding of these and structurally similar molecules, like Tsr to tyrosine, chemotactic activities have been observed and become a basis for further study (Hazelbauer et al., 2008).

Tsr has been the receptor of focus in recent experimentation due to recent demonstrations that of epinephrine, norepinephrine, and indole bind tightly as ligands. Norepinephrine and

epinephrine are catecholamines which are synthesized in the adrenal medulla, which is located on the kidneys in the mammalian host, and function as hormones through the body, and epinephrine/norepinephrine work as neurotransmitters in addition in neuron synapses (Cervi et al., 2013). The role of these and further neurotransmitters in the gut are associated with regular inflammation and muscle contraction throughout the gastrointestinal tract (Lomax et al., 2010), and regulate bacterial chemotaxis through the Tsr.

QseCB, upon binding to ligands such as the AI-2 or nor/epinephrine, leads to the degradation of norepinephrine and an increase in the concentration of DHMA in the bacteria's immediate surroundings. Tyramine oxidase, *tynA*, tyramine oxidase, and aldehyde dehydrogenase, *feaB*, work to synthesize 3,4 -dihydroxymandelic acid (DHMA) from norepinephrine, which increases the growth of gram-negative bacteria (Lyte et al., 1992). More recently, DHMA has been demonstrated as a ligand for Tsr and functions as a moderately strong chemoattractant (Pasupuleti et al., 2017).

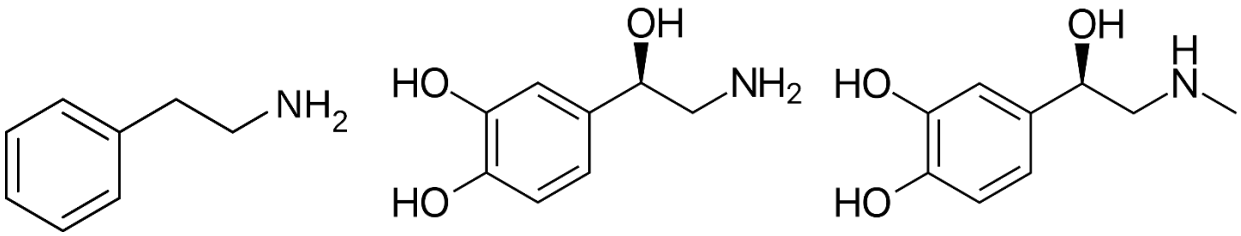

Figure 2*:* ß-Phenylethylamine, Norepinephrine, and Epinephrine Molecules. Norepinephrine and epinephrine are known ligands of the Tsr and are both derived from tyrosine. ß-Phenylethylamine, a trace amine, has similar functional groups to norepinephrine, including a terminal amine.

It is hypothesized that the space with relatively high DHMA concentration functions as a chemoattractant in a quorum-like fashion for bacteria swimming through the intestine, and lead bacteria such as *E. coli* to the surface of the intestinal epithelium for congregation into a biofilm community (Lyte et al., 1996). In addition, this DHMA promotes the expression of virulence

associated genes on the locus of enterocyte effacement (LEE pathogenicity island) in EHEC (Sule et al., 2017).

Chemotaxis to Gut-Associated Lymph Tissues (GALTs)

Mammalian physiology is dependent on homeostatic regulators which control metabolic activity in specific tissues and influence the activity of skeletal muscles in addition of autonomic contraction (Kawashima, 2005). Peyer's patches, which are hubs of lymphoid, nervous, and respiratory systems, and are typical targets of enterocyte effacement (Phillips et al., 2000). These patches, known generally as GALTs, are atypical in the intestine for the fact that they, despite the function of the intestine to absorb nutrients, secrete and release monoamines from these enteric nerves (Meirieu et al., 1986). Monoamines found in the intestine are numerous, but of interesting note is the common synthesis of catecholamines and trace amines by commensal bacteria that may impact human-derived compound concentrations (Clemente et al., 2012).

A class of molecules which exist in the intestine in trace amounts are the trace amines, many of which are derived from amino acids, similarly to the neurotransmitters of the catecholamine family and serotonin (Kuroki et al., 1990). One such trace amine of interest is ß-phenylethylamine (PEA), which is a trace amine known to function in conjunction with dopaminergic neurons in the central nervous systems (Mercuri et al., 1997). Though the relative concentrations of PEA are found to be nearly two-three orders of magnitude lower than that of dopamine in the neuron synapses, its function is considered integral to the overall functions of dopamine release and the inhibition of dopamine uptake ins the CNS, though is also present throughout the nervous system (Ishida et al., 2005). At high concentrations, it has also been shown that PEA degradation products have a distinctive destabilizing effect on bacterial cells' ability to grow biofilms (Horne et al., 2018).

Seeping of catecholamines and some trace amines is most likely a result of the leaky nature of the Peyer's Patches, which function in the education of the immune system by frequent exposure to ingested materials (Reboldi et al., 2016). Further, human enterochromaffin cells found lining the intestine are the major source of serotonin synthesis in the body are a source for other metabolites which are secreted into the intestinal lumen (Furness et al., 2013). Perhaps surprisingly, the connections between neurotransmitter synthesis in the intestine, along with close connection with blood and lymph tissue, may lead directly to chemical changes in the brain (Bellono et al., 2017). This proposed gut-brain connection via the neural and respiratory systems is a matter of recent human-bacterial studies.

As genomic analyses progress, further progress has been made in associating commensal bacteria and their impacts on the mammalian host (Qin et al., 2010). The evolutionary relationships between commensal gut bacteria and mammals may reveal further the role of bacteria in the host's metabolic processes in the microbiome studies (Sudo, 2019). In addition, the impacts of new and potentially pathogenic microbes may also be interpreted based on the changes observed in the gut microbiota (Bäumler et al., 2016). Following the theme of the impacts on bacterial physiology as relates to human physiology, the interaction of bacteria on surfaces with human neurotransmitters, especially regarding intestinal colonization.

E. coli Biofilm Formation in the Presence of Neurotransmitters

Biofilms are defined as bacterial colonies encased in a matrix that forms on surfaces, liquid-atmosphere interfaces, or within eukaryotic cells (Costerton, 1995). The ability of bacteria to attach to their position on a surface is mediated by curli and fimbriae, and perhaps pilin (Carter et al., 2016). In addition, cyclic AMP concentrations serve functions as secondary messengers in the initiation pathway for many bacterial species (Römling et al., 2013). The

previously mentioned EnvZ, OmpR, and RcsCDB influence *flhD* transcription and impact the formation of biofilm through biofilm associated cell organelles (Gottesman, 1991) Structures such as flagella are integral in the initial foundation of biofilm on surfaces such as the intestinal wall, from which further maturation may proceed (Giron et al., 2002). As the biofilm grows, an increase in the number of bacteria is needed to gain a concentration of AI-2 to stimulate QseCB in these cells, inducing further biofilm formation as well as the expression of various virulence factors (Gonzalez et al., 2006).

Priyankar Samanta, previously a student in the Pruess laboratory at NDSU, engineered pPS72, or a *flhD::gfp* fusion plasmid, which was constructed using a cloned fragment containing the *flhD* promoter from *E. coli* AJW678. This promoter containing region begins 1,419bp upstream of the +1 transcriptional start site and ends 502bp downstream of that same site. This *flhD* promoter region is inserted into a pUA66 vector immediately upstream and in-frame of *gfpmut2* and makes pPS72 into a reporter that expresses GFP following transcriptional events activating the *flhD* promoter. This construct allows for transcribing *gfp* relative to the activation of the *flhD* promoter, providing a benchmark for relative *flhD* transcription. This will be integral to gauge relative transcription of *flhD* specific transcription as indicated by the fluorescence observed as a byproduct.

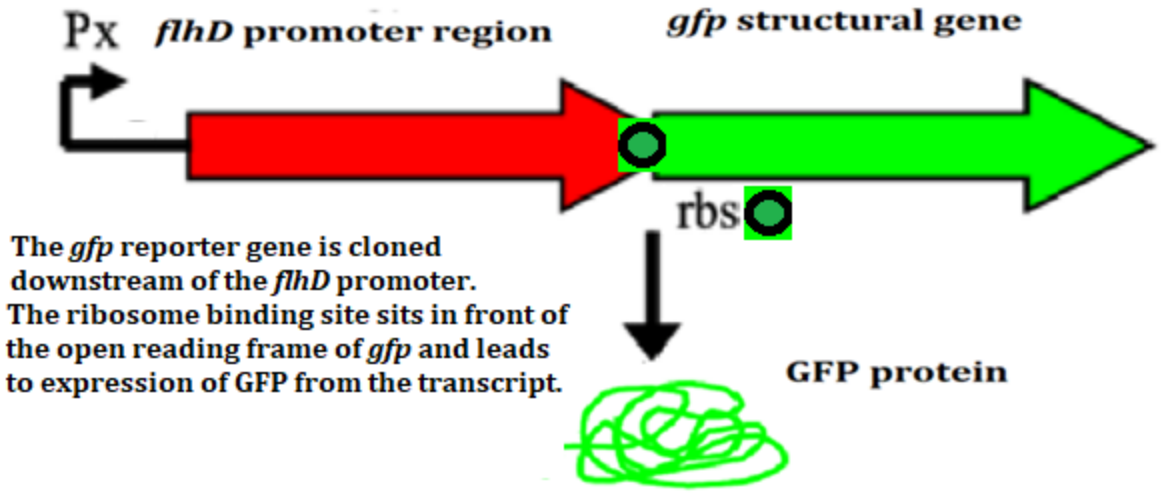

Figure 3: The pPS71 Fusion Mechanism. By adding the *flhD* promoter to the *gfpmut* containing plasmid, activation of the *flhD* promoter will directly transcribe *gfp,* which is translated via the rbs into GFP protein, and observable by fluorescent microscopy.

Biofilms pose serious health risks, as many pathogens depose themselves and create colonies which constantly serve as a reservoir for the disease's causative agent (Wong et al., 2000). The polysaccharide capsule encompassing these biofilm colonies may also provide a physical barrier against the host's immune system as well as rapid distribution of anti-microbial compounds (Ryan et al., 1986). Bacterial biofilms often cause diseases in the human body and other mammalian hosts, but bacteria are also capable of attachment to inorganic surfaces and may serve to transfer contamination from the environment into the new host, as in the case of catheters (Rasamiravaka, 2015). This knowledge has led an effort the study biofilms for potential treatments to bacteria protected by forming films.

Questions and Research Goals

It is apparent that the activity of catecholamines function to stimulate the flagellar operon. Activity of QseCB also indirectly leads to a buildup of chemotactic agents which may then function to attract further bacteria to a niche, once flagellar genes have been expressed and a full flagellar apparatus has been built. Once bacteria have begun the process of biofilm formation, catecholamines may further contribute to the maturation of said biofilms.

Bacterial chemotaxis is attracted to particular compounds which may be found in the human intestine. The full list of molecules which exist in the intestine and may stimulate chemotactic activity is not entirely known, and likely includes chemotactic agents not yet described. Microorganisms which utilize their hosts' own neurotransmitters or serve to synthesize neurotransmitters may have an important role in the chemotactic signals in the gut, and can offer insights in the complicated interplay of these species and their molecular arsenals.

The use of ß-phenylethylamine has been useful in disrupting processes in bacteria such as *E. coli, S. aureus, P. aeruginosa,* and others in their biofilm communities in limiting general growth in pharmaceutical products (Hasan et al., 2019). ß-phenylethylamine also shows similar functional chemistry with the other ligands of QseCB and Tsr and it may also be susceptible to modification by *E. coli* enzymes, TynA and FeaB, to degradation into Phenylacetic acid (PAA). PAA has been shown to disrupt TypeIII secretion systems in *P. aeruginosa* (Wang et al., 2013) If ß-phenylethylamine can bind QseC and stimulate *flhD* transcription, it may directly affect the growth of biofilm. If these enzymes can modify ß-phenylethylamine into a form which binds strongly to Tsr, similarly to DHMA from norepinephrine, or whether it binds without modification, ß-phenylethylamine may stimulate chemotaxis.

The questions of this study were then formulated: does ß-phenylethylamine affect the ability of bacteria to form biofilm through *flhD* transcription, and what chemotactic effects does ß-phenylethylamine induce in *E. coli*? The following was hypothesized: PEA will function to inhibit the ability of *E. coli* to form biofilm, and PEA will act as a chemoattractant compound. To answer these questions involves testing *E. coli* bacteria with ß-phenylethylamine and other similar neurotransmitters under 24-hour long treatments to measure the resultant biofilms formed and to determine the relative *flhD* expression. Secondly, we wish to determine whether ß-phenylethylamine stands as a potential chemoattractant agent for bacteria through two assays. With this information, in addition to the information gain from other common catecholamines found in the human intestine, we may be able to identify previously undescribed biofilm stimulating molecules as well as some novel chemoattractant.

MATERIALS AND METHODS

Bacterial Strains

Bacterial strains utilized for this study are summarized in Table 1 and include four non-pathogenic *E. coli* strains. The *E. coli* strain utilized for *flhD* transcription and biofilm testing experiments was *E. coli* AJW678 transformed with pPS72 and labeled as BP1553. AJW678 is noted for growing a robust biofilm (Kumari et al., 2000), and the plasmid PS72 contains the *flhD* promoter from AJW678 fused to the gene for green fluorescence protein (*gfp*) on plasmid pUA66 (Samanta et al., unpublished). *E. coli* MC1000 is a strain of highly motile bacteria (Castilho et al., 1984) transformed with an *ompC*::*gfp* containing plasmid for constitutive *gfp* expression (Keio collection: http://cgsc2.biology.yale.edu/), listed as BP1431. BP1431 was used for the plug agarose motility assay for its rapid production of flagella. MC1000 Δ*flhD*::*kn* (Malakooti 1989) was transformed with pAS Red2 and used as a non-motile control for plug agarose assay as a Brownian-motion control and in the microfluidic device assay as a basepoint for digital calculations. RP437 has been used previously as the motile strain for microfluidic device assays (Parkinson, 1978). This strain carried the GFP expressing plasmid pMC18 (Hansen et al. 2001).

Bacterial strains were stored and maintained as -80°C freezer stocks in 8% dimethyl sulfoxide (DMSO). *E. coli* cultures were prepared by plating from freezer stock onto Luria Bertani agar plates (10 g/l tryptone, 5 g/l NaCl, 5g/l yeast extract, 5g/l agar), supplemented with the appropriate antibiotic and dosage. Inoculated plates were incubated at 37°C overnight. Liquid overnight cultures were prepared from plate colonies by picking isolated colonies and inoculating into respective liquid media fortified with antibiotics.

Table 1: Bacterial Strains

Strain Collection ID Number (BP)	Genotype	Notes	Reference
AJW678	*AJW647 proC+ ΔlacX74 = thi-1 thr-1(Am) leuB6 metF159(Am) rpsL136 ΔlacX74*		Kumari et al., 2000
BP1553	AJW678 pPS72 *flhD*::*gfp*	For *flhD* transcription and biofilm experiments	Samanta et al.
MC1000	F-, *ara*D139 Δ(*araAB leu*)7696 Δ(*lacX74*) *galU galK strA prsL thi*		Castilho et al., 1984
BP1431	MC1000 *ompC*::*gfp*	Motile strain for plug agar assays	This study
MC1000 *flhD::kn*	F-, *ara*D139 Δ (*araAB leu*)7696 Δ(*lacX74*) *galU galK strA prsL thi*		Malakooti et al., 1989
BP1605	MC1000 *flhD*::*kn* pAS Red2 amp^R	Non-motile strain for plug agar assays and microfluidic assays	This study
RP437	F-, *thr-1*, *araC14*, *leuB6*(Am), *fhuA31*, *lacY1*, *tsx-78*, *λ*$^-$, *eda-50*, *hisG4*(Oc), *rfbC1*, *rpsL136*(strR), *xylA5*, *mtl-1*, *metF159*(Am), *thiE1*		J.S. Parkinson, 1978
RP437 pCM18		Motile strain used in microfluidic device assays	Hansen et al. 2001

FlhD Transcription Assay.

To determine transcription of *flhD,* AJW678 pPS72 (BP1553) was grown in an overnight culture in tryptone broth (TB, 10 g/l Tryptone, 5 g/l NaCl) at 34°C supplemented with 25µg/mL Kanamycin. The overnight culture was transferred into a conical tube and centrifuged for 10 minutes at 15°C and 4500 rpm in an Avanti Benchtop Centrifuge. The resulting pellet was resuspended in 10mL PBS and this suspension was centrifuged for 10 minutes at 15°C and 4500rpm. The resulting pellet was resuspended in fresh TB (with 25µg/mL Kanamycin) and diluted with such to an OD_{600} of 0.05. This culture was then transferred into wells of a 24 black-well plate. The wells were then supplemented with some concentrations of neurotransmitter. Twelve concentrations of neurotransmitter in TB were replicated twice in each plate, at 0, 0.1, 0.5, 1, 5, 10, 50, 100, 250, 500, 750, and 1000 µg/ml. This plate layout was reproduced in three biological replicates resulting from individual colonies from the petri plate, yielding a total of six technical replicates for each treatment concentration. The neurotransmitter molecules used for this study included ß-Phenylethylamine (PEA), dopamine (DOP), epinephrine (EPI), norepinephrine (NOR), and serotonin (SER). Plates were sealed and inserted into the Synergy H1 Hybrid Reader and incubated at 34°C for 24 h. The plate was programmed to measure OD_{600} and relative fluorescence at an excitation/emission wavelength of 485/521nm on an hour interval for this 24-hour period to determine growth and *flhD* transcription at specific timepoints. Following the read, the plate was discarded, and the data was exported to an Excel document for analysis.

Crystal Violet Biofilm Assay

Crystal violet (CV) assays were used for the quantification of *E. coli* biofilm. AJW678 pPS72 (BP1553) was grown in an overnight culture in TB at 34°C supplemented with 25µg/mL Kanamycin. 10µL of this culture was then inoculated into each well of 24 polystyrene plates in 1ml TB treated with one concentration of neurotransmitter, in a similar fashion to the preceding *flhD* transcription experiment. Plates were then sealed and incubated at 34°C for 24 hours. Following incubation, plates were emptied of planktonic cells and excess media, and the wells were rinsed lightly with PBS three times to remove non-adherent bacteria and excess media. After an hour-long drying period, wells were stained with 0.1% CV solution for 15 minutes. The excess stain was then rinsed from the wells with PBS three times, and the plates were dried for 1 hour. The stained organic material was then extracted with an 80/20 ethanol/acetone solution for 5 minutes, and 150 µl of extracted CV was transferred to each well of a 96 well polystyrene plate. The OD_{600} of these extractions was read using the Synergy H1 Hybrid Reader and exported to an Excel document and the plate was discarded.

ATP Biofilm Assay

ATP assays for the quantification of viable biofilm. AJW678 pPS72 (BP1553) was grown in an overnight culture in TB at 34°C supplemented with 25µg/mL Kanamycin. 10µL of this culture was inoculated into each well of a 24 well polystyrene plate in 1ml TB treated with one concentration of neurotransmitter, in a similar fashion to both preceding experiments. Plates were then sealed and incubated at 34°C for 24 hours. Following incubation, plates were washed thrice lightly with PBS to remove planktonic bacteria and excess media. Remaining bacteria were then homogenized in 1 ml PBS, triturating to break up adherent cells into solution. 100 µl

of this homogenized bacterial suspension was pipetted into one well of a 96 well Greiner white plate. 100 µl of BacTiter-Glo™ reagent was then added to each well. The plate was placed on a rotating shaker for 5 minutes and was then read by the Synergy H1 Hybrid Reader for resulting luminescence. The data was exported to an excel document and the plate discarded.

Plug Agarose Assay

E. coli MC1000 Δ*flhD* pAS and MC1000 pOmpC::gfp and were grown overnight separately in TB at 34°C with 50 µg/ml kanamycin or 100 µg/ml Ampicillin, respectively. These cultures were inoculated 1:40 into new TB the following morning and then were incubated at 34°C until to an OD_{600}=0.5. 1 ml of each culture was centrifuged at 400rpm for 10 minutes. This pellet was washed in each tube using 0.5 ml chemotaxis buffer (CB; 1X PBS, 0.1 mM EDTA, 0.001 mM l-methionine, 10mM DL-lactate). Both tubes were then rotated at 120 rpm while held at 34°C for 10 minutes in an orbital shaker. Lightly resuspended cultures were combined into a single tube using a wide-bore pipette tip and gently mixed by inversion.

To prepare the agarose plug, 950 µl chemotaxis buffer, 20 mg of low melt agarose, and chemoattractant (serine or PEA) at concentrations of 0.5 mM, 1 mM, or 5 mM were mixed. To each solution, 50 µl of saturated bromophenol blue solution was added and the contents of the tube melted together. 5 µl of this molten mixture was pipetted onto a glass microscope slide for each assay. Supports made of 10µL plain CB/agarose were placed onto the microscope slide on either side of the plug. A glass coverslip was then laid over the supports and plug, leaving a small space under the coverslip above the slide. It was recommended to prepare the plug agarose during centrifugation and rotation of bacterial cultures.

50µl-75µL of prepared bacterial culture containing both strains was pipetted gently under the coverslip and incubated for 30 minutes at 34°C. Slides were then imaged under fluorescent

microscope under FITC and TRITC filters to generate images of GFP expressing motile bacteria and RFP expressing non-motile bacteria, respectively.

Microfluidic Motility Assay

Methods for the Microfluidic chemotaxis assay have been previously described by Sule N et al., 2017 with one alteration: instead of using antibiotic killed, RFP expressing TG1 cells, RFP expressing, non-motile MC1000 were substituted. Cells are prepared as described by Mao H et al., 2003.

Microflow devices were fabricated by use of a laser-lithography method which produced an imprint of the device onto a silicon wafer. These silicon wafers were employed as molds for the imprints of the channels through the device. A poly(dimethyl)siloxane (PDMA) material was mixed and poured onto the silicon wafer mold and allowed to cure. Glass microscopy slides were cleaned using isopropanol and acetone and set aside for oxygen-plasma bonding. Devices were removed from the silicon wafer mold and access ports were pushed through the PDMS material using a semi-sharp 19-gauge needle. Fitting silicon tubing of approximately 18 inches in length were placed ¾ of the way into the PDMS ports, or until firmly attached to minimize any leaks of breaks. The PDMS device is then adhered to cleaned and oxygen plasma treated glass slides to ensure air-tight seal. Onto the silicon tubes, disposable syringe attachments were inserted, and syringes filled with CB with added neurotransmitter compound were attached to the outer two inlets, avoiding introduction of air bubbles.

Cells were prepared similarly to the protocol described for the plug agarose assay, substituting RP437 pCM18 for BP1431. Colonies pulled from plates stored short-term in refrigeration of BP1431 and BP1605 were grown overnight at 34^{o}C in TB with Erythromycin (25µg/mL) and Ampicillin (100µg/mL) added, respectively. Cell cultures were diluted 1:10 into

appropriate antibiotic fortified media and grown to an OD_{600} of 0.5. Cultures were then diluted 1:5 at a volume of 5 mL each and centrifuged at 400rpm for ten minutes. Following centrifugation, supernatant was disposed of, and 0.6 mL of CB was added to each culture. The cultures were resuspended gently in a rotator device for ten minutes at 30^{o}C. RFP expressing cells were then transferred into the GFP expressing culture, and this solution was gently mixed by slight inversion. The combined bacterial culture is attached to the central inflow inlet.

The neurotransmitter and culture prepared device were placed into the flow chamber and attached to the PicoPlus programmable pump and microscope apparatus. Flow of the pump achieved a volume of 5µL/minute, and images (FITC, TRITC, and regular light) were taken once every second for 100 seconds for analysis.

Data Analysis

Data from the *flhD* transcription experiments were analyzed from three biological replicates and two replicates of each biological replicate for a total of six replicates. The replicates for fluorescence were divided by the corresponding replicates for $OD_{600.}$ The final timepoints (Fluorescence/OD_{600}) were chosen for this analysis. These values were analyzed by One-Way ANOVA for variation from the value of the control samples ([0]) at the 25-hour reading. Data points were determined significant at p-values <0.05 by Least Square Means (by t-distribution) and Dunnett's test with adjusted *p*-value utilized to gauge significance. The averaged value of the 25-hour timepoint with error bars determined from standard deviation were plotted for each concentration.

Data from the Crystal Violet and ATP Biofilm Assays were analyzed from three biological replicates and two replicates of each biological replicate for six total replicates. Data points were analyzed by two-handed Student's *t*-test to determine significance compared to the

control. Data points from each concentration averaged together represent the bars in the plots, and standard deviation values were used for error bars.

Data images from the Plug Agarose assays were analyzed qualitatively for patterns of congregation on the agarose plug, comparing with the activity observed in the control plug.

Data images from the Microfluidic Device Assays were analyzed by the bCount Software as described in detail in Pasupuleti et al. 2017. Pixel counting software counts GFP and RFP expressing bacteria in the picture of the cell and determines a line of best fit from the RFP bacteria. Variance in the GFP from this line of best fit bacteria may be calculated and determines a value for the Minimum Motility Coefficient. Images of the compiled snapshots for GFP and RFP are displayed along with the MMC values.

RESULTS

FlhD Transcription Assay – Neurotransmitter Treatment Shows E. coli Response

In order to identify the impact of neurotransmitters on the transcription of *flhD*, an assay was performed to quantify the total of such by the parallel expression of fluorescence by Green Fluorescing Protein by means of a *gfp::flhD* fusion.

Determination of statistical significance (indicated by the asterisk above the significant datapoint) was determined by Least Square Means (LSM) and Dunnett adjustment for multiple comparisons with an adjusted *p*-value of $p \leq .05$ as significant.

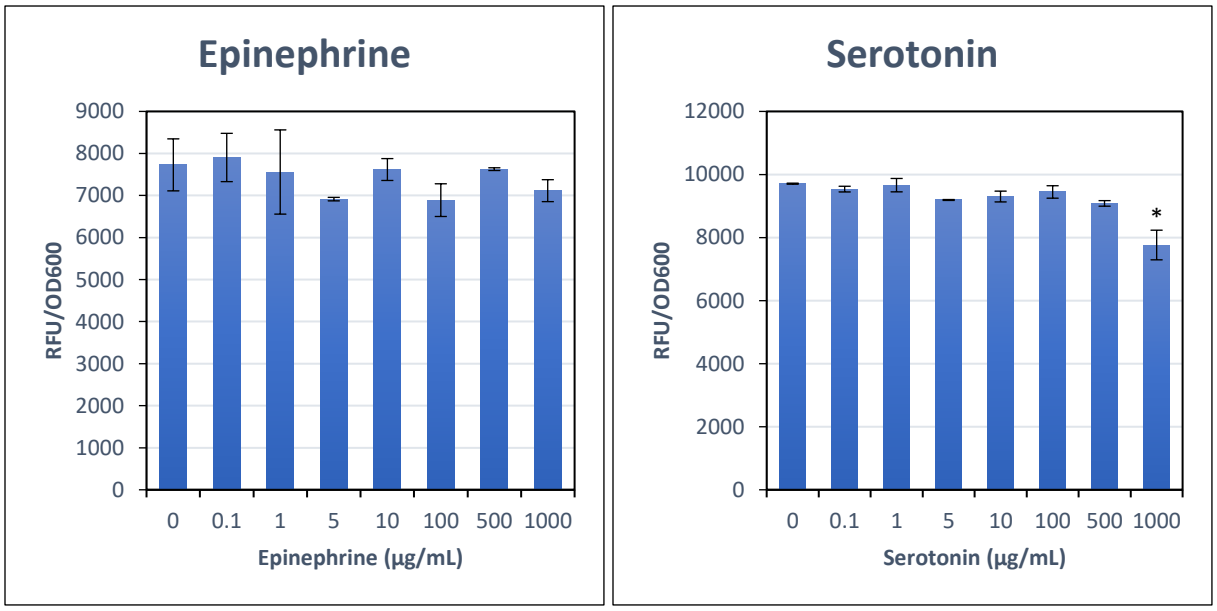

Figure 4: Epinephrine and Serotonin *flhD* Transcription Data. Neurotransmitter treatments on *E. coli* AJW678 pPS72 *flhD*::*gfp* yielded fluorescence and optical density data for samples at each concentration. The bars represent the averaged fluorescence/OD_{600} for each concentration at the 24 hour reading mark. Significance is represented by the * and is found by analysis with LSM and Dunnett with significance determined at end adjusted *p* values $p \leq .05$.

Treatment of *E. coli* AJW678 pPS72 with epinephrine of AJW678 pPS72 *flhD*::*gfp* at concentrations of 0.1 µg/mL to 1000 µg/mL yielded no significant differences of relative *flhD*

transcription from bacteria treated with no epinephrine. No significant biological indicators may be inferred, and the data would indicate no pattern indicating change with dosage.

Treatments with serotonin yielded a decreasing pattern of relative fluorescence with increasing concentration of serotonin, with the 1000 µg/mL causing a 34.5% reduction of growth and a 58.8% reduction in *flhD* transcription, or 20.1% reduction in relative *flhD* transcription. Further testing at higher concentrations showed more defined reductions in both growth and *flhD* transcription, and may indicate some strong effects on the bacteria's survival linked with the serotonin concentration.

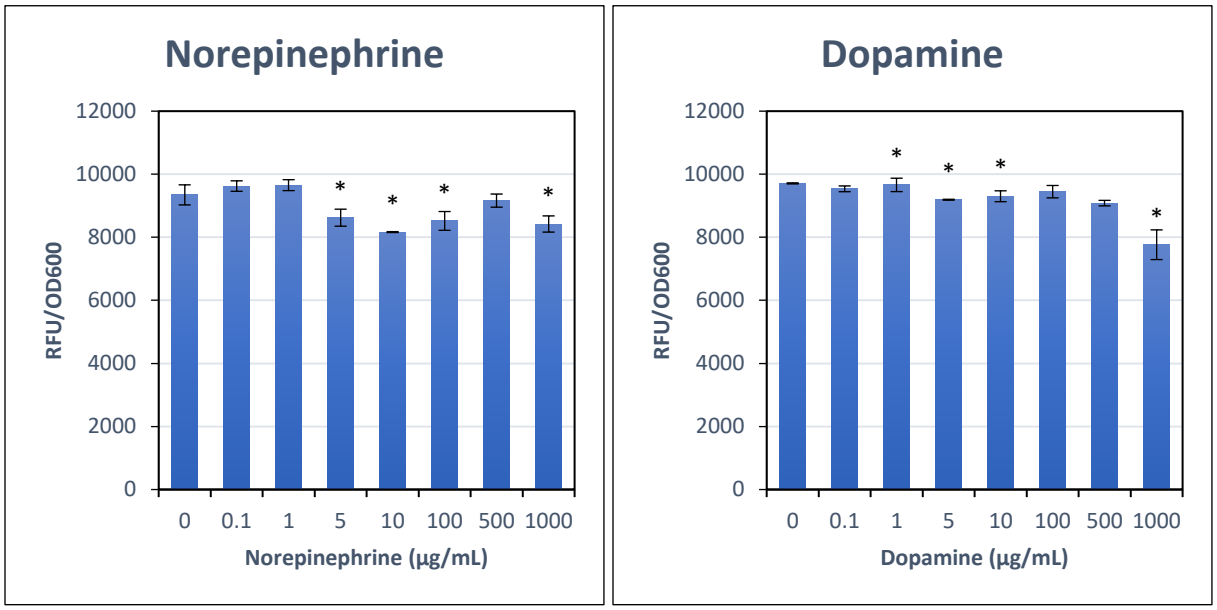

Figure 5: Norepinephrine and Dopamine *flhD* Transcription Data. Neurotransmitter treatments of *E. coli* AJW678 pPS72 *flhD*::*gfp* yielded fluorescence and optical density data for samples at each concentration. The bars represent the averaged fluorescence/OD_{600} for each concentration at the 24 hour reading mark. Significance is represented by the * and is found by analysis with LSM and Dunnett with significance determined at end adjusted *p* values $p \leq .05$.

A pattern of a dip may be seen with some treatment concentrations from the 5µg/mL-100µg/mL range. The norepinephrine treatments of 5 µg/mL-100 µg/mL and 1000 µg/mL reveal statistically significant reductions compared with the zero, but the difference in growth at the high concentration (1000 µg/mL) may suffer from the toxicity issues.

Dopamine treatment at increasing concentrations demonstrate a sharp decline from the control, with relative transcription of *flhD* dropping in the highest concentrations tested. The treatment of 1µg/mL-10µg/mL and 1000µg/mL do show significance difference, but the difference in growth at the high concentration (1000µg/mL) may be due to the tendency of dopamine to oxidize under a near neutral pH, creating a pigment that may influence OD_{600} readings. The pigment does not appear to be visible to the naked eye in concentrations lower than 500µg/mL. The changes at the high concentration may also imply observable differences in the ability of the bacteria to grow, when looking for biological patterns underlying the data for the 1000µg/mL treatment group. Regardless of the pigmentation, the data do trend in a downward direction with the increase of Dopamine, and reveals relatively less transcription.

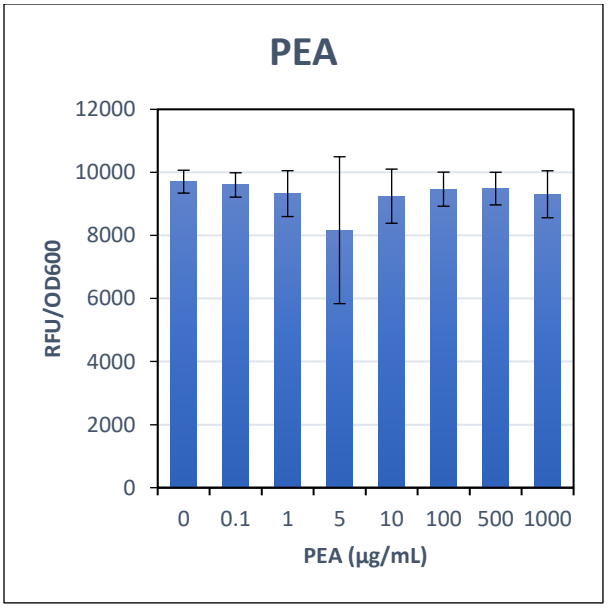

Figure 6: PEA *flhD* Transcription Data. PEA treatments on *E. coli* AJW678 pPS72 *flhD*::*gfp* yielded fluorescence and optical density data for samples at each concentration. The bars represent the averaged fluorescence/OD_{600} for each testing concentration at the 24 hour reading mark. Significance is represented by the * and is found by analysis with LSM and Dunnett with significance determined at end adjusted *p* values $p \leq .05$.

PEA treatments at concentrations from 0.1µg/mL to 1000µg/mL caused no statistically significant difference of relative *flhD* transcription from the zero concentration. The widest observed variations could be found in the datapoints at 5 µg/mL concentrations, for which many samples showed much reduced transcription data. The standard error may cast doubt on the likely biological significance; the variation may show some effect on the bacteria leading to the high error relative to the other treatment groups.

Crystal Violet Biofilm Assay – Neurotransmitter Treatment Shows Biofilm Mass Impact

To quantify the formation of biofilms under the influence of neurotransmitter treatments, BP1553 bacteria were placed with neurotransmitter and grown for 24 hours. The resulting biofilm was stained, the crystal violet dye was solubilized, and then transferred into a 96 well plate and read in the plate reader at OD_{600}.

The data points from each replicate were averaged and are represented by the bars in the graphs in Figures 6 to 10. The data points were used to determine standard deviation, which are represented by the error bars in the same graphs. Significance was determined by variance from the [0] dataset by two-handed Student's *t*-test with significance determined at end values $p \leq .05$.

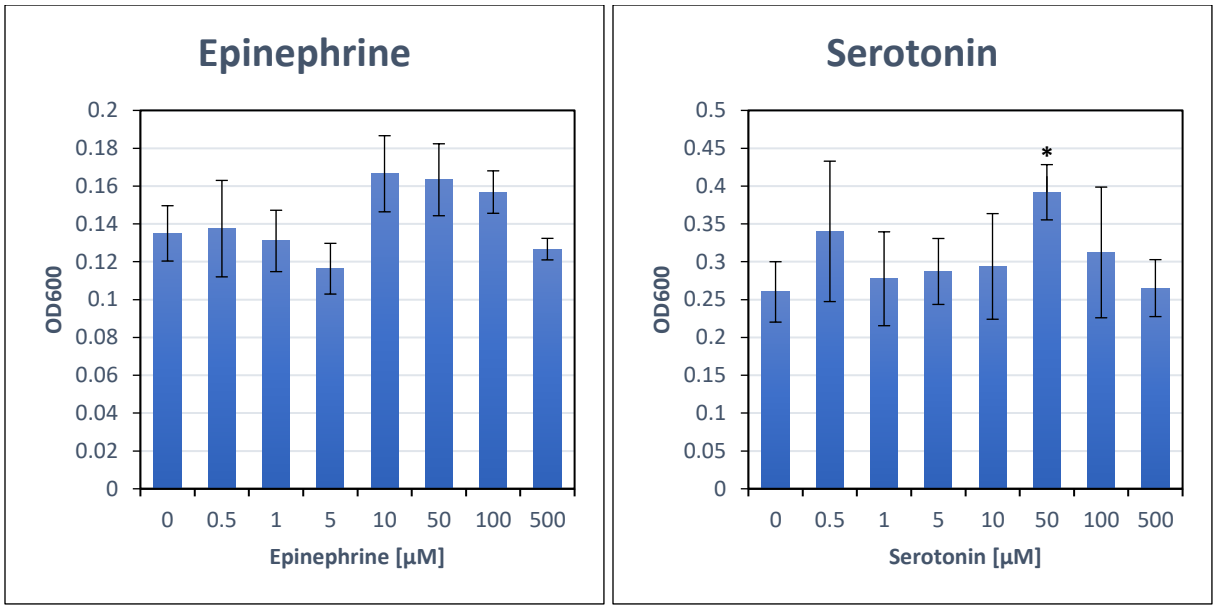

Figure 7: Epinephrine and Serotonin Biofilm Data. Neurotransmitter treatments of *E. coli* AJW678 pPS72 *flhD*::*gfp* yielded optical density data for samples at each concentration. The bars represent the averaged OD_{600} for each testing concentration at the 24 hour reading mark. Significance is represented by the * and is found by two-handed Student's *t*-test with significance determined at end values $p \leq .05$.

The averaged optical density from the samples treated with epinephrine at concentrations of 0.5-500 µM fall closely to the values of the samples without epinephrine treatment. Mass of biofilm then trends on higher values starting with 10µM at 23.3% increase from the zero, but then begins to taper off taper off at the higher concentrations, which may reveal decreases in bacterial survivability as biofilm amounts drop below the zero. The spike at 10µM does not appear to have any observable indicators in the previous concentrations as they increase.

Samples treated with serotonin show peaks at 0.5µM at a 30.7% increase and 50µM at a 50.4% increase, surrounded by gentle increases and decreases. No uniformity in the other serotonin treatments are shown to be significantly greater or lesser than in the [0] conditions. The statistical analysis shows the increase measured in the 50 µM samples to also be of a significant increase, from which the peak then descends into biofilm mass comparable with the control. The rise in the 0.5µM is also notable for showing a similar trend rising towards and then decreasing

away in what may appear a bimodal fashion. These peaks are unique among serotonin, with the highest demonstrable changes in biofilm mass of all the tested concentrations.

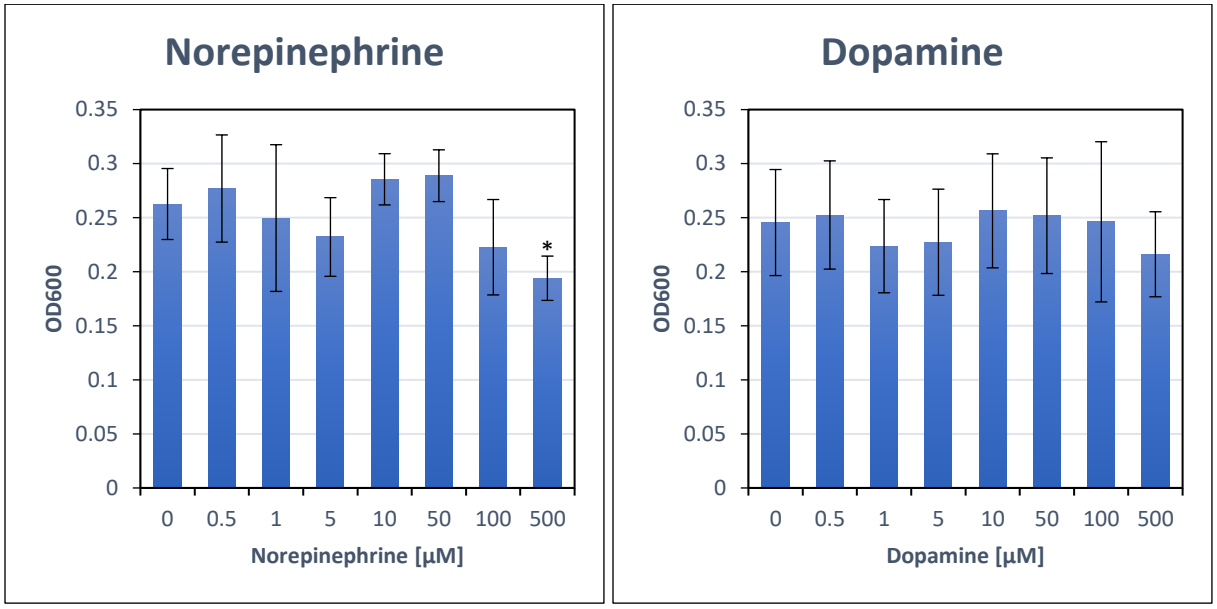

Figure 8: Norepinephrine and Dopamine Biofilm Data. Neurotransmitter treatments on *E. coli* AJW678 pPS72 *flhD*::*gfp* yielded optical density data for samples at each concentration. The bars represent the averaged OD_{600} for each testing concentration at the 24 hour reading mark. Significance is represented by the * and is found by two-handed Student's *t*-test with significance determined at end values $p \leq .05$.

The samples treated with 500 µM norepinephrine demonstrate a significant decrease of from the [0]. Starting from the 50µM concentration, a distinct decrease forms as concentration treatment increases to drop over 25% of mass. The biofilm can be macroscopically seen to diminish as the concentration of the Norepinephrine increases following the staining procedure, and falls demonstrably beneath its low concentration and control counterparts. A smaller dip is observed at 5µM, but then the biofilm quantity raises to levels similar to the [0] by the 10µM.

Samples treated with dopamine did not exhibit great variance from the [0] across all tested doses. Pigmentation occurred during the incubation of the dopamine treatments but did not seem to impact the formation of a biofilm when compared with the [0]. All resultant biofilms fall

into a similar range, indicating Dopamine having little role in increasing or lowering total amounts of biofilm.

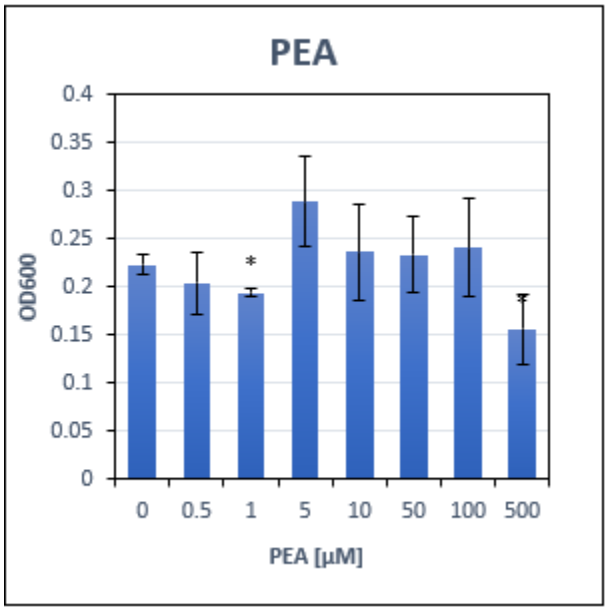

Figure 9: PEA Biofilm Data. Neurotransmitter treatments of *E. coli* AJW678 pPS72 *flhD*::*gfp* yielded optical density data for samples at each concentration. The bars represent the averaged OD_{600} for each testing concentration at the 24 hour reading mark. Significance is represented by the * and is found by two-handed Student's *t*-test with significance determined at end values $p \leq .05$.

The treatments of PEA at 1 µM and 500 µM showed statistically significant reductions by comparison to the [0]. From 5µM, a strong increase can be observed of a 29.5 percent increase, followed by decline that intensifies sharply at 500µM PEA. The drop in optical density at the 500 µM concentration shows the strongest reduction observed in biofilm, which may bear strong semblance to data derived in work done by Horne et al., 2018, and Irsfeld et al., 2013. Further increases in concentration may show an effect of greatly diminishing the bacteria's ability to form films.

ATP Biofilm Assay – Neurotransmitter Treatment Shows Little Impact on Biofilm Metabolism

To support results of the Crystal Violet Assay, the ATP Biofilm Assay was implemented to quantify the metabolic activity of biofilms under the influence of neurotransmitter treatments. BP1553 bacterial biofilm was solubilized, treated with BacTiter Glo, and read under luminescence fiber to gauge relative metabolic activity.

Significance was determined by variance from the [0] dataset was found by two-handed Student's *t*-test with significance determined at end values $p \leq .05$.

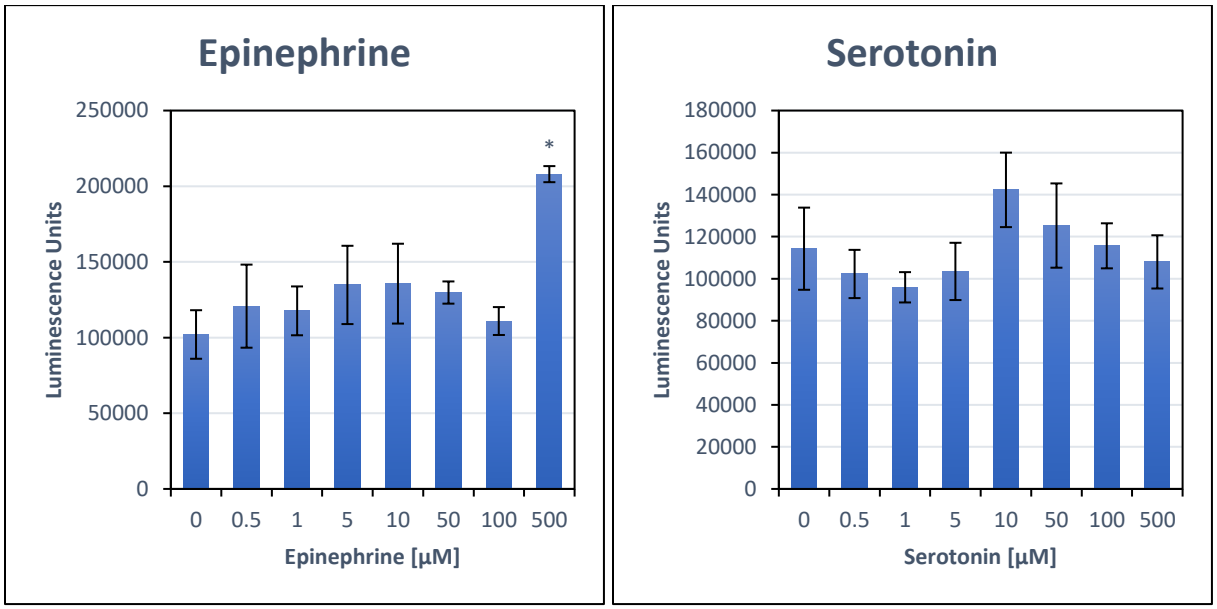

Figure 10: Epinephrine and Serotonin ATP Data. Neurotransmitter treatments of *E. coli* AJW678 pPS72 *flhD*::*gfp* yielded luminescence data for samples at each concentration. The bars represent the averaged luminescence reading for each concentration at the 24 hour reading mark. Significance is represented by the * and is found by two-handed Student's *t*-test with significance determined at end values $p \leq .05$.

The averaged data from the samples treated with 0.5-100 µM fall similarly to the samples without epinephrine, yet the 500 µM shows significantly higher viability that the [0]. These data points appear to be outliers which may have affected the samples. The general and steady

increase followed by a steady rate of decrease may indicate where epinephrine may function as a nutrient and as antimicrobial to the bacteria, respectively.

Samples treated with serotonin did not show any statistically significant increase or decrease across all concentrations for viability. The value achieved at the 10µM concentration shows a height increased from the zero by 24.5% followed by a steady decrease as the concentration increases. Again, a low point near the 5µM then leads to a large increase by the seemingly abrupt 10µM. From there, the data descend gradually to the level of the control.

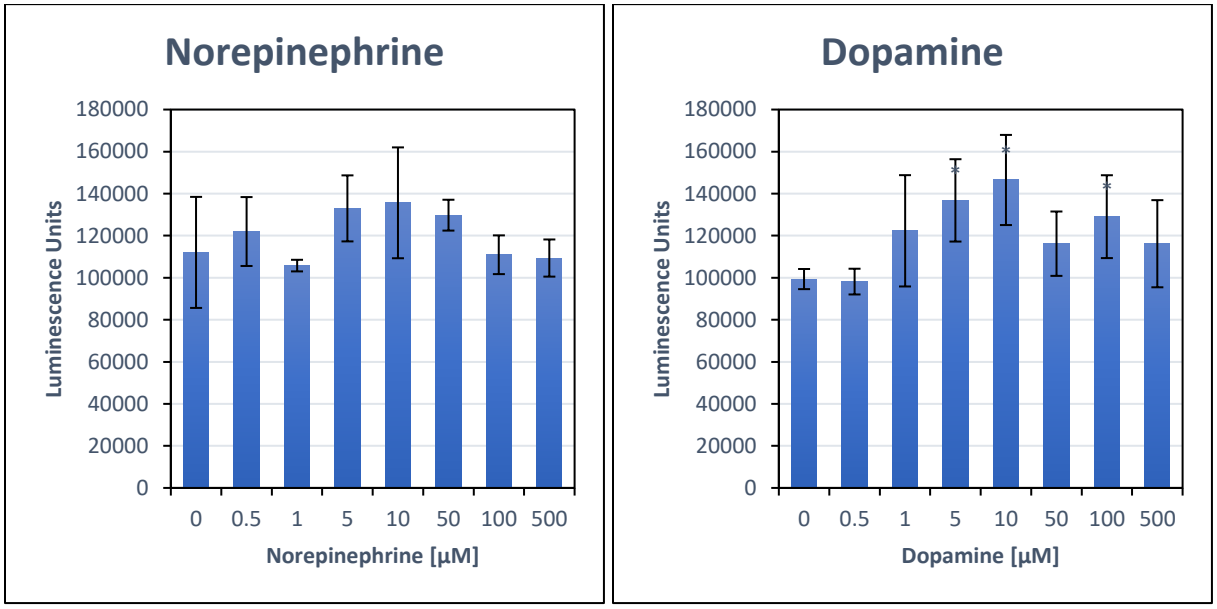

Figure 11: Norepinephrine and Dopamine ATP Data. Neurotransmitter treatments of *E. coli* AJW678 pPS72 *flhD*::*gfp* yielded luminescence data for samples at each concentration. The bars represent the averaged luminescence reading for each concentration at the 24 hour reading mark. Significance is represented by the * and is found by two-handed Student's *t*-test with significance determined at end values $p \leq .05$.

The norepinephrine treated samples show a small "dip" at the 1µM treatment, but then a small "bump" from 5µM to 50µM. Statistically, there are no changes from no Norepinephrine, and biologically, there is no difference that would strongly distinguish any group of samples. High concentrations appear similar to the control following the high points observed at intermediate doses.

In contrast, the variation on the samples from the dopamine treatments at 5, 10, and 100 µM all show significant statistical increases from the [0] of 37.6%, 47.4%, and 29.9%, respectively. Treatments between 1µM and 10µM demonstrate and increasing pattern, and at 50µM demonstrate a definitive decrease. The increases may lead to even more cell representation in the physical biofilm compared to the zero, which may also have strong effects on the metabolic state of the constituent bacteria in that biofilm. The highest concentrations also maintained a higher ATP measurement than the [0] though without a definitive trend. The peak of this unimodal peak appears to be at 10µM.

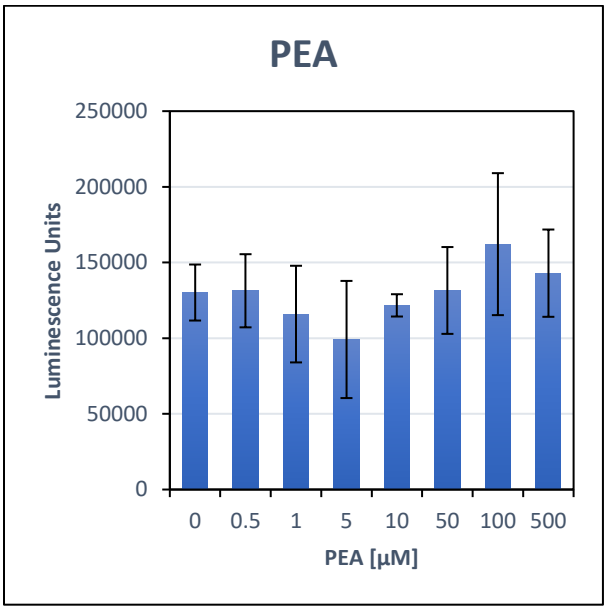

Figure 12 : PEA ATP Data. Neurotransmitter treatments on *E. coli* AJW678 pPS72 *flhD*::*gfp* yielded luminescence data for samples at each concentration. The bars represent the averaged luminescence reading for each concentration at the 24 hour reading mark. Significance is represented by the * and is found by two-handed Student's *t*-test with significance determined at end values p≤.05.

The PEA treated samples did not show any significant differences from the [0]. A "dip" may be inferred from 1µM to 5µM, then increasing above the controlled sample datapoint. Immediately at 10µM, the data trend upward, again reaching levels that are similar in scope to the [0] and an increase of up to 24.6% in the 100µM. The biological changes are not so

pronounced as to distinguish any one group over another, once error is considered, which is larger than in previous experiments in this section.

Plug Agarose Assay – Treatments of PEA Indicated Chemoattractant Properties

To initially qualify the chemotactic influence of PEA on bacteria, the plug agarose assay placed both motile (BP1431) and non-motile (BP1605) *E. coli* in a small chamber with an agarose plug containing some chemotactic agent. After a brief incubation period, the chamber was viewed under fluorescent microscope to observe either uniform distribution of bacteria, indicating no net chemotaxis, or congregation of the bacteria on the interface of the agarose plug, indicating net chemotaxis to the PEA containing plug. Results were determined to show chemotaxis based on relative comparison with the control treatment (plain agarose plug).

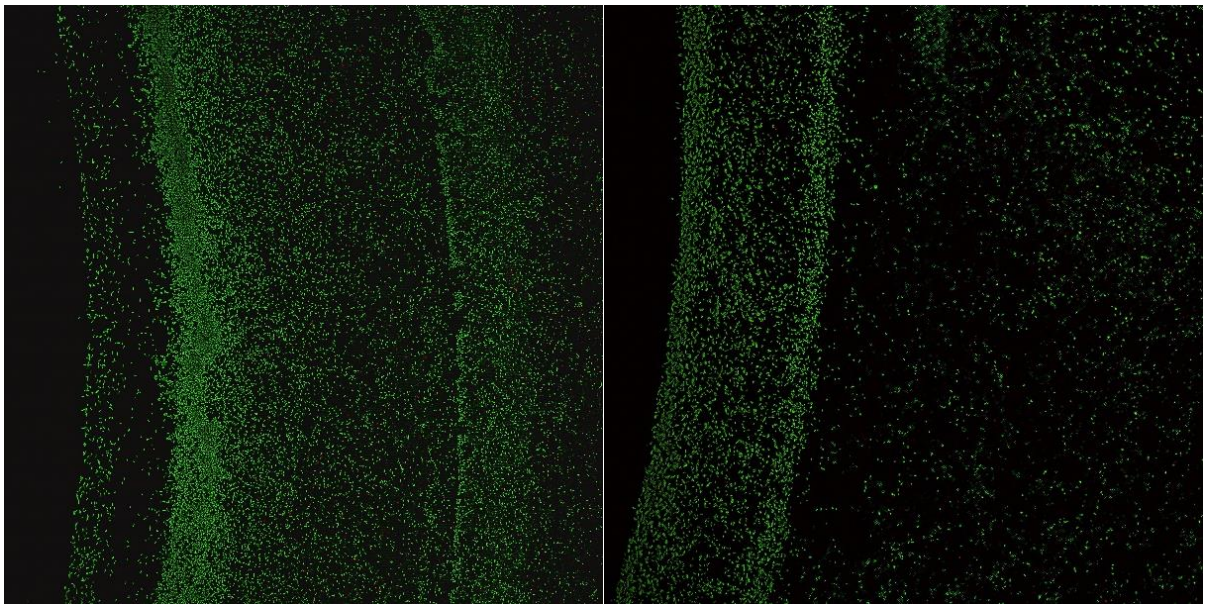

A B

Figure 13: Serine (A) and PEA (B) Plugs at 5 mM. (Agarose plug on the left) The right side of the image shows GFP expressing bacteria suspended in CB. Some visible differences in bacterial concentration may be observed as distance from the plug surface increases.The relative number of bacteria on the plug surfaces compared with the bacterial suspension is indicative of non-negligible chemotaxis.

The 5 mM Serine plug with heavy concentration on the plug surface indicates strong chemattractant properties of serine. Further bacteria may be observed to the right, but is clearly decreasing concentration compared to the highly congested slope of the plug.

The 5 mM PEA plug may indicate some low to moderate chemoattraction, showing a large relative numer of bacteria near to or on the plug's surface compared to swimming through the liquid medium. The lower number of bacteria routinely observed at this concentration may also indicate a lack of strong chemoattraction.

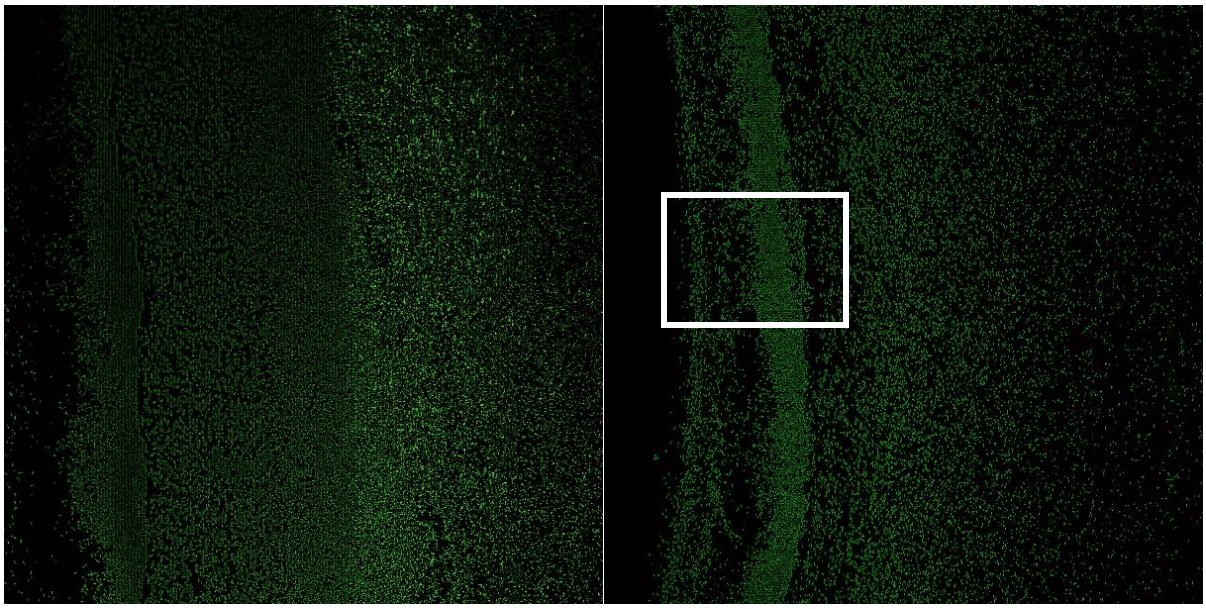

A B

Figure 14: Serine (A) and PEA (B) Plugs at 1mM. (Agarose plug on the left)

Observable concentration of bacterial cells exists on the surface on the Serine plug, forming a large lawn across the plug's surface. Decreasing cell density further from the plug supports the observation of congregation and chemoattraction to the surface. The 1 mM PEA shows increased attraction from the higher 5 mM PEA, with visible congregation of bacteria forming a thick smear covering the plug's surface on the left third of panel B (indicated by the white box). Dosage dependence appears to factor into the ability for PEA to attract the bacteria.

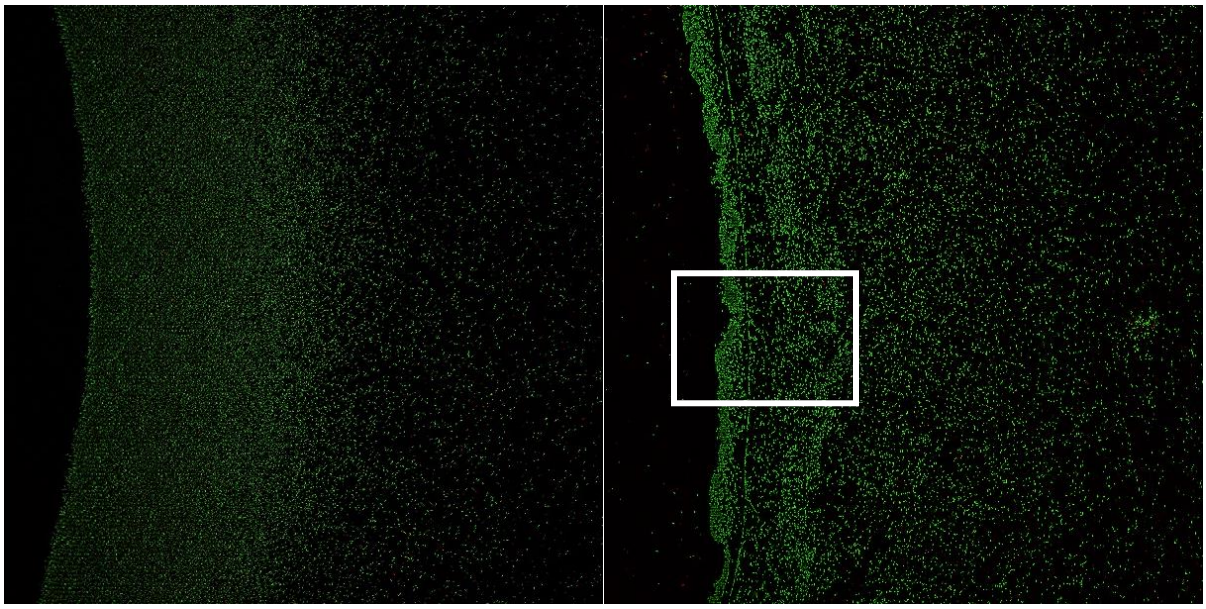

A B

Figure 15: Serine (A) and PEA (B) Plugs at 0.5 mM. (Agarose plug on the left)

0.5 mM serine causes mitigated chemoattraction totally surrounding the plug for a wide distance. Strong chemotaxis to the plug is a likely analysis of serine even at a concentration of lower magnitude. The concentration of bacteria further from the plug is clearly dramatically lower than in the area surrounding the plug.

0.5bmM PEA causes chemoattraction comparable to concentrations of 1 mM PEA demonstrated in the previous figure. Though a strong congregation of bacteria adere to the surface of the 0.5 mM PEA plug (as seen in the white box), the concentration of the bacteria in the observable field to the right side may indicate a dwindling effect of dosage. There is very likely chemotaxis to the plug, but of a sort that does not create a clear disparity in bacterial concentration that is easily recognizable in the serine plugs.

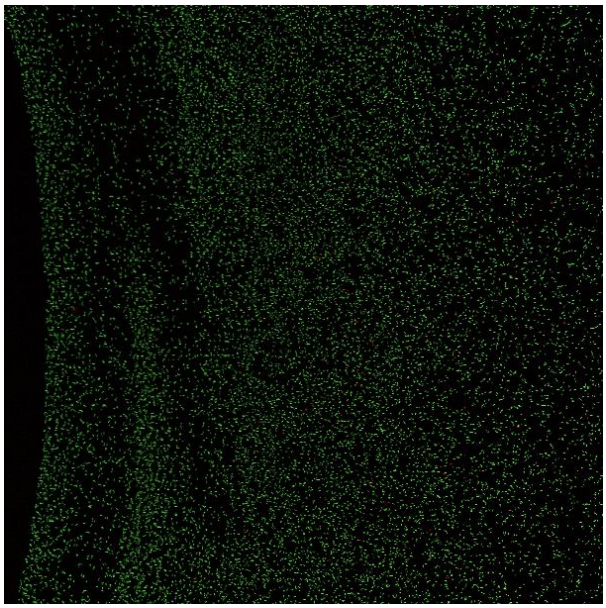

Figure 16: Control Plug.

The bacteria seen through the negative control (**Figure 4**) are evenly distributed throughout the entirety of the liquid environment. The lack of any bacterial congregation implies that the buffer control does not show any definitive chemotaxis Similarly, there is no congregation that may be associated with handling during the imaging process, which may have skewed the image result. Another important function of the control is the define the edge fo the agarose plug, as it is a three-dimensiol surface on which the *E. coli* may fall.

The comparison of the control with serine at 5 mM and 1 mM show large differences in the congregation of the bacteria on the surface of the agarose plug, as well as the area immediately adjacent to the plug in PEA at 1µM and 0.5µM concentrations and serine at concentrations of 5µM, 1µM, and 0.5µM. PEA does not immediately show high levels of chemotattraction at the 5 mM concentration, but a decrease in concentration to 1 mM and 0.5 mM show a definitive congregation of bacteria, indicating chemoattraction. The agarose plug and surrounding environment in the 5 mM are very similar to the chemotaxis buffer control with a field of fairly undisturbed bacteria steadily in the foreground, but for the 1mM and 0.5mM

PEA samples, the plug surface becomes strongly lit by fluorescing bacteria. The fields in the 1mM PEA samples also show a decrease in the even concentration of bacteria that are found in the immediate area of the plug, indicating that the bacteria are being pulled while within a certain distance of the plug.

Microfluidic Motility Assay – PEA Demonstrates Quantifiable Chemoattractant Properties

The microfluidic assay was employed to determine a specific and quantifiable chemotaxis. Pictures were taken at excitation frequencies for both GFP and RFP and were conglomerated. The analysis of the photos was conducted through a shape-counting program, bCount, which calculates the relative positions of each red RFP non-motile and each green GFP motile bacterium. The RFP shapes were used to calculate a line of best fit, and the distance from this line to each GFP shape was averaged on the left and right sides, then these two numbers were averaged together. This number is the MMC, or the minimum motility coefficient. This number describes the intensity of chemotaxis toward test chemicals.

By placing *E. coli* RP437 pCM18 and BP1605 into a flow of plain chemotaxis buffer, serine, and PEA, values gauging chemotactic behavior were derived by the relevant software.

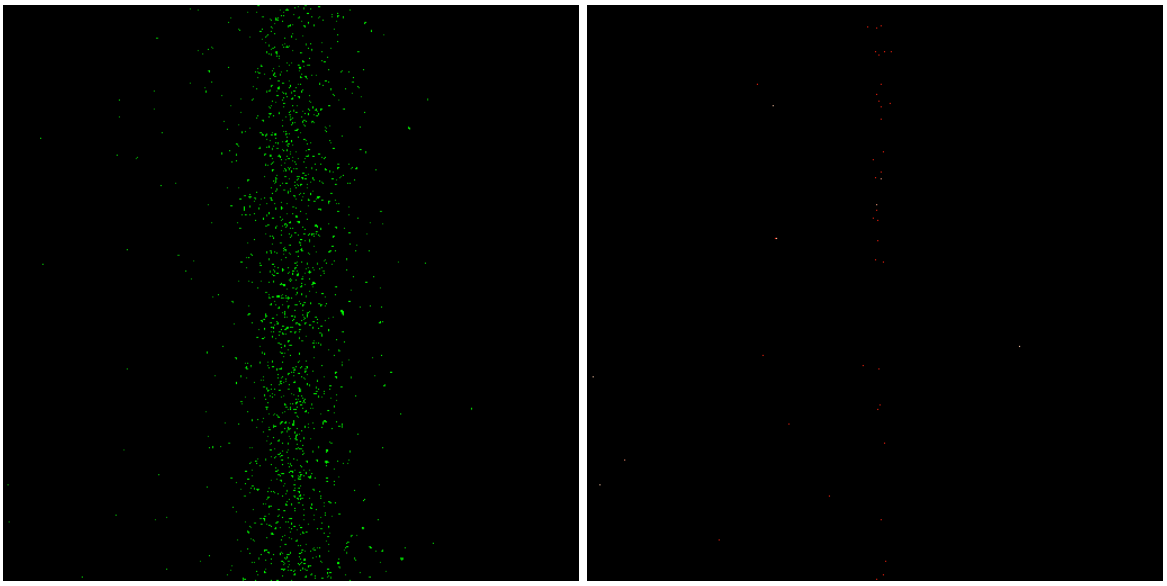

A B

Figure 17: Chemotaxis Buffer Negative Control Microfluidic Assay. GFP (A) and RFP (B) expressing bacteria. The spread of the GFP expressing bacteria is calculated by the line of best fit determined by the RFP expressing bacteria. Though difficult to spot, some small read bacteria can be seen flowing through the center of panel B.

The pictures are taken in such a manner that the edge of the channel is found at the edge of the image on the left and right sides. Through the chemotaxis buffer control (negative), motile GFP bacteria are concentrated at the center of the channel, with some spread to the left and right ends of the chamber. The spread can observable be limited to the center of the image.

The nonmotile RFP bacteria are sparse, yet can be seen predominately in the center of the image in panel B. The tight pattern of the nonmotile bacteria is qualitatively indicative of a lack of directional movement from the central flow in the chamber, and any movement from the flow would likely be stochastic in nature. Similarly, the impact of external forces, such a Brownian motion, or responses to fluorescent light are thus accounted for in the final comparison.

Following analysis of the bCount software, the chemotaxis buffer control resulted in an MMC value of 0.0793472, which is classified as neutral regarding chemoattractant effect. This would indicate the buffer has a negligible effect on the chemotaxis through the flow chamber.

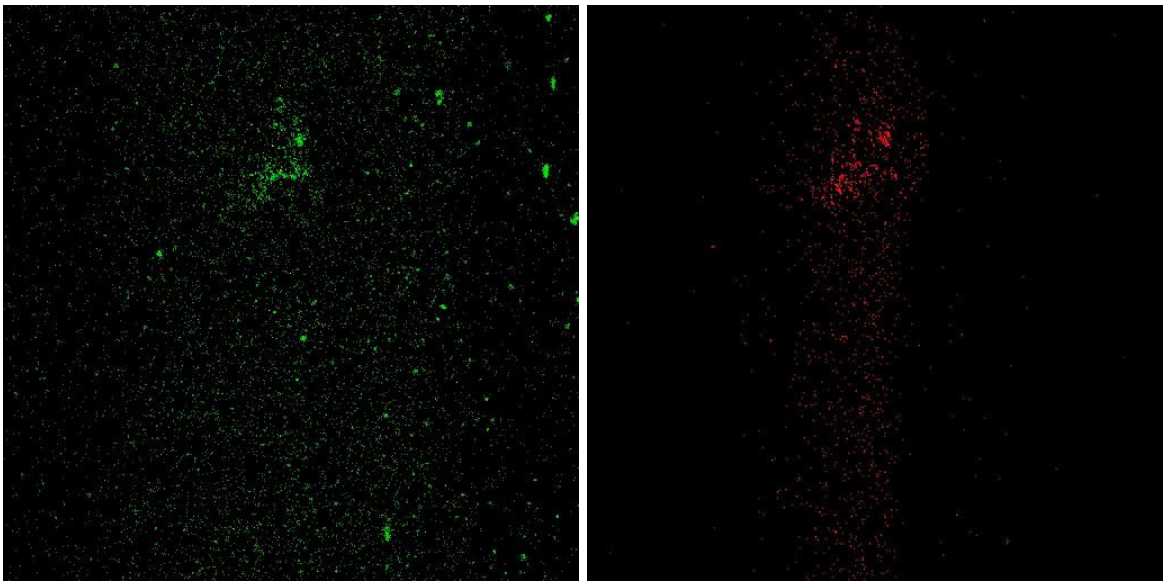

A B

Figure 18: Serine Positive Control Microfluidic Assay. GFP (A) and RFP (B) expressing bacteria. Serine, a documented chemoattractant associated with the Tsr receptor, is used as a positive control to determine if the GFP expressing bacteria can chemotax in presence of known chemoattractants.

Spread of the GFP expressing motile bacteria in panel A reaches to the very edges of the chamber on both the right and left sides of the chamber. Though many bacteria may be seen near the middle of the chamber, the almost regular looking spread of bacteria shows a distribution covering the majority of the chamber. This is indicative of chemotaxis from the less concentrated serine in the middle of the chamber to the more concentrated serine concentrations found in the edges of the flow.

The nonmotile RFP expressing bacteria are here more well represented in the flow chamber in panel B. Though there is an observable spread of the RFP expressing bacteria, it looks to be contained to the middle of the chamber. It may be helpful to compare **Figure 18B** to **Figure 17A** to compare the expected flow of non-chemotaxing bacteria of a similar number. It should be noted that, though having more red bacteria may be useful, only a few bacteria need be

observed by the program to determine a line of best fit, with more bacteria leading to a slightly more accurate line.

Clusters of bacteria may indicate some minute imperfections in the chamber, which may lead to odd flow and distinctive channels forming. The lack of a defined channel is useful evidence to support the validity of this test. The motile bacteria are qualitatively further from the center of the channel and indicate activity on the part of the bacteria to lead away from the central direction of flow. The nonmotile bacteria, in contrast, still sit to the center of the chamber, showing no disruption of the direction of the flow.

Following analysis by the bCount software, the serine positive control resulted in an MMC value of 0.415973. This value demonstrates wide range for motile bacteria reached in the chamber, which is consistent with strong chemotactic activity in the motile bacteria.

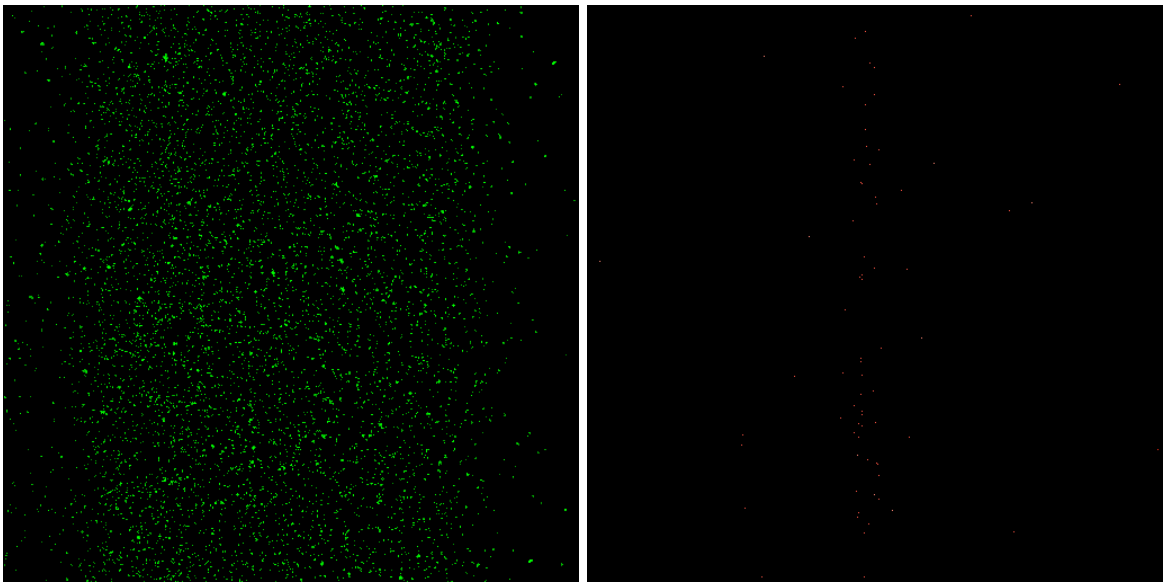

A B

Figure 19: PEA Microfluidic Assay. GFP (A) and RFP (B) expressing bacteria. PEA, better known as a nutrient source (Horne et al.) is being tested to quantify chemotaxis it may cause in bacteria. Again, a low concentration of RFP expressing bacteria in panel B is difficult to observe, but not prohibitive for the analysis software.

The GFP expressing motile bacteria can be clearly seen across the near entirety of the chamber. In comparison with **Figure 18 A**, one may see that there are some small differences in the totality of the spread, most notably, the distinctive "drop" in GFP expressing bacteria to be found on the very edges of the chamber. Though slightly less fully spread than serine, the PEA chemotaxis can be observed to be of a much higher magnitude that of the chemotaxis buffer control by simple side by side comparison.

The RFP expressing nonmotile bacteria, though more sparse than in **Figure 18 B**, still can be made out in the center of the chamber in **Figure 19 B**. As in the earlier figures, the RFP bacteria remain near the center of the chamber and do not resist any flow from the center. The difference between the spread of the GFP and RFP bacteria in **Figure 19** is arguably more stark than the previous assays by quick visual analysis.

The PEA microfluidic assay shows a wide range in the motile bacteria, yielding an MMC value of 0.356306. This value is considered normal for chemo-attractive effects, when taken with earlier publications of the assay. Although there are several known chemoattractive agents, serine is one of the strongest chemoattractants. By comparison, PEA's MMC value of 0.356306 may be safely described as having definitive chemoattractant qualities.

Table 2: Minimum Motility Coefficient

	Chemotaxis Buffer (-)	Serine (+)	PEA
MMC Value	0.0793472	0.415973	0.356306

The control for the microfluidic device created a standpoint by which to judge the basic dispersion of *E. coli* in comparison to a known chemoattractant (serine). The analyzed data was formed from a single run each of a control, a serine, and a PEA based assay. The images and

datasets were selected after a decision to use the RP437 strain bacteria in lieu of our MC1000 strain used in the plug assay for initial images taken earlier.

The minimum motility coefficient of 0.5 would indicate a perfect spread of motile bacteria across the chamber, and a coefficient of 1.0 to indicate all motile bacteria against the far walls of the chamber. By achieving a value much closer to 0.5 than to our “stagnant” value of 0.079, PEA may be considered a chemoattractant as a result of comparing the MMC values.

DISCUSSION

In summary of the data, we see clearly that the presence of the various neurotransmitter compounds has produced some effect in each particular field. Regarding dosage effects on the transcription of *flhD*, the rapid relative decrease in transcription can be seen in increasing doses of Serotonin and Dopamine. In biofilm deposition, the experiment's intermediate doses showed increases in the quantity of biofilm as compared with lower and higher doses in Epinephrine and Phenylethylamine, but no consistent changes in Serotonin, and notable decreases in Norepinephrine and Dopamine treatments across dosing. The biofilm's metabolic activity showed notable increases at intermediate concentrations between 5µM and 50µM in Norepinephrine, Serotonin, and Dopamine, but relatively more moderate change in Epinephrine in these same concentrations, and a near opposite trend of a decline at intermediate levels in Phenylethylamine. Chemotaxis showed promising trends which then illustrated strong chemotactic effects toward Phenylethylamine in comparison with Serine.

The transcription of *flhD* revealed a remarkable effect, namely in Serotonin and Dopamine: though moderate dosage showed no great effect on transcription, a relatively high concentration of these two neurotransmitters moderated a severe decline in the transcription of *flhD*. Through this data we can glean that these two neurotransmitters have a similar effect and may imply a similarity in the mode of action of these molecules on the bacteria's transcriptional regulation. The quickly discernable difference of the totally unobstructed amine found which is found at the tail of these molecules, but not found in the others, may be a contributing factor that leads to similar binding on some MCP, and thus may explain results that nearly mirror one another in the data. As the other treatments did not engender the same activity, I believe the similarities of these molecules would be the most likely method of explaining those like results.

A more specific dosing of these treatments could be utilized to expand on the similarity of this relationship, and how far in concentration this relationship holds true.

The formation of biofilm paints a new picture in which results in Epinephrine, Serotonin, and Phenylethylamine show a change in the moderate dosing of the neurotransmitters. Consistently in Phenylethylamine and Epinephrine, we observe that the moderate concentration of the treatments lead to a distinctive rise in the resultant biofilm which then tapers out as concentrations rise. Serotonin displays some increases across all treatments, but to spot a defining trend proves tricky, and so inferring a mode of action may not be simply stated. Although a bimodal distribution looks reasonable in Serotonin and Norepinephrine, testing into more specific concentrations in that relative concentration range would likely elucidate whether there are two peaks on maximum biofilm formation surrounding two concentrations in particular. Norepinephrine and Phenylethylamine also demonstrate a meteoric decline at the higher concentrations, which may imply some lethality in this dosing. The mode of action by which these molecules influence the biofilm may be more complicated to describe than via the *flhD* network, and may depend on factors not examined directly in this study.

As for the metabolic activity gauged, it is apparent that the treatments of the neurotransmitters less Phenylethylamine all demonstrated increases, and these increases typically show a single concentration in contrast with the bimodal data observed in the earlier mass gauged. Some showed gradual raises, such as Epinephrine and Norepinephrine, towards their moderate dosing. The other found a more dramatic rise, as found in Dopamine and Serotonin in the moderate doses. Only in Phenylethylamine do we observe some instance of a decline, which then bounces back to control level metabolism at the higher doses. This seems interesting in the cases of the four treatments that increased as opposed to the one that decrease, as perhaps the

presence of the treatments at a moderate dosing allowed for some nutrient or positive stimulation, but that the moderate dosing of the other perhaps played the role of a toxin or antagonist to regular metabolism.

In observation of chemotaxis, results of the plug-in-pond assay revealed that accumulation of bacteria is distinctive in comparison with the “empty” plug and the positive control. Further, a specific concentration of PEA appeared to induce more optimal chemotaxis, which may indicate a dosage dependency. The subsequent testing performed in the microfluidic device revealed definitive quantitative chemotaxis which gauged positively in comparison with a known chemotactic attractant.

The results have added to our current understanding of the relationships between neurotransmitter molecules and the transcriptional behaviors of *E. coli* in reaction. Most interestingly, relatively high doses of the neurotransmitters Dopamine and Serotonin prove to change the net balance of *flhD* transcribed per bacterium present in the system in a *downwards* trend. In a system where a nutrient or other beneficial molecular is present, a decline in flagellar development may be a useful evolutionary strategy to minimize energy expended in motile behavior as well as maximize niche adaptation (Pruess, 2017). The high concentration of these two neurotransmitters may play a role in preparing the bacteria for a transition to a sessile state, though it this assertion may not hold strongly with the data found in the actual creation of biofilm, as other neurotransmitters appear to more strongly encourage this activity as well, and even more strongly in some cases. Though the particulars of this mechanism may be dependent on more than the mere concentration of the neurotransmitters, the fact that the same changes could not be found in the remaining treatments would imply different means of effecting the bacterium, such as the activity of untested autoinducers which may alter physiology by quorum

activated in a related two-component system (Gonzalez et al, 2006). A future venue to explore the underlying mechanics could be a study to determine the strength of binding between Dopamine and Serotonin to various MCPs which send along messages in the form of transcriptional regulation.

Similarly, physiological changes in the *E. coli* bacteria also vary with the dosage of the specific transmitters show differing biofilm follows treatments of neurotransmitters, but in contrast with the *flhD* regulation, appear to show most concentration changes near the middle of the chosen dosing regimen. For Epinephrine, Serotonin, and PEA, a moderate dosing appeared to most positively influence the accumulation of biofilm, but relatively low and high concentrations show similar quantity development to the control. This may imply that only stimulation in a certain concentration may lead to the signal transduction, triggering the change in the biofilm's deposition. This may be an evolved mechanism to deliberately control the allocation of cell resources towards to construction of energy-inefficient extracellular matrix in conditions where either the advantages of rewards are either too low, or that it would be more efficient to remain in a more free planktonic form, due to the relatively high and stable concentration of the external nutrient. This and other resource allocation systems may be coupled with the stressors that involve EnvZ, OmpR, and RcsCDB, which directly impact this system further upstream (Gottesman, 1991)

The data from the metabolic representation of biofilm testing showing the increased metabolic activity at these middle-dosage points would also perhaps glean some understanding in the pattern – that, under the optimal conditions where biofilm formation may be optimal under some steady but median neurotransmitter signal, was found that the metabolic functioning of the bacteria was also higher. This would support the possibility of the inputs towards formation of

matrix may be the result of a finely calculated evolutionary pressure, of which the reception of the signal by the MCP may be finely tuned towards optimal survivability as regulated by cyclic di-GMP (Römling et al., 2013). In this, the data for the Epinephrine and Serotonin seen in total mass of biofilm would be explained by the advantages in the doses. Again, here as in the *flhD* activation, the specification of the MCP and relative strength of binding may illuminate more clues as to a verifiable mechanism such as was sought after in research spearheaded by Sule et al., 2017.

Of the chemotactic study, the information derived is less than complete, but provides a fine clue as to mechanisms in addition to behavior. The chemotaxis found on the plug was novel in its own right, describing PEA's potential as an attractant for *E. coli*, yet these is still room for confirmation of the testing by nature of the single successful attempt of the microfluidic device described here. One result that surprised the author was that the concentration of PEA tested for the single functioning assay achieved strong chemotaxis in *E. coli* – an area of research considered important for future study by other researchers in motility (Sourjik et al, 2013). This indication that the concentration at which chemotaxis is observed is similar in several molecules that stimulate the bacterium, like as was the case in DHMA, and so optimal concentrations of other molecules to test may be attempted in the same concentration ranges (Pasupuleti et al., 2017).

The mechanism for chemotaxis is well known, but the identity of molecules that may stimulate the MCP and at what strength in concentration dependency remains an open question, even if these results help to narrow the band (Karavolos et al., 2013). But even with this knowledge, variables which went here untested may disproportionately impact the result, such as the role of the memory functioning in chemotactic activity as well as the resulting relative signal

amplification of the cytoplasmic elements that influence flagellar rotation (Parkinson et al., 1979). This can offer a clue into the role of concentration into the activity it encourages in the bacterium – a very high concentration of neurotransmitter may function to *minimize* smooth-swimming and to promote tumbling, all of which acts as a simplistic physiological feedback loop to turn off chemotaxis when advantageous. Suffice to say, it is clear that the attraction the *E. coli* tested demonstrates toward PEA is quantifiable at the concentration tested. The mechanism through the TSR and the near homologous nature of the molecules known to bind the receptor were clues to the possibility of dimerization of this MCP and signaling by this mechanism (Milligan et al., 1988).

The roles of the neurotransmitters on *E. coli* are certain, and signal transduction is believed by the author to be at the root of those mechanisms. A direction into the specific rate of binding, dimerization, and subsequent transcriptional regulation/physiological reaction would be the means by which to flesh out the likely sources of the variations found by each of those neurotransducers. Of curiosity, though many of the molecules have differing effects, most of the tested neurotransmitters were of fairly similar molecular composition, usually differing from any other by a single functional group. The activity of each of these under different physical conditions, may also be useful to discern different environments in which these may have some effect. For example, performing testing at a physiological pH of 7.0 may have limited those neurotransmitters with a lower half-life under such conditions.

There are a few notes to be discussed here for correction and contemplation upon further testing of these chemical and biological relationships. The testing performed was done under conditions that were physiologically suitable to the bacteria tested, under the hope that the effects of the neurotransmitters as treatments would be clearly discernable. In some ways, the results are

acceptable as a basis for greater study, in that the relationships described here now have a strong basis for validation by other means. In some other ways, the efficacy of these tests done *in vitro* may be precluded by accurate description *in vivo*, as the circumstances under which these interactions may take place in nature are bombarded by unknown bacteria, molecules, temperatures, levels of pH, and so on.

A matter of importance for some of the molecules tested is in the limited stability they have at a regular physiological pH, as the environments in which they are found either see degradation and constant input into that system, or of a decidedly lower pH, as evidenced in the intestinal lumen of mammalian species. Even more intriguing is the presence of enzymes in the intestine, both from bacteria and other microbes, which may degrade these neurotransmitters and therefor alter the molecular composition of the environment and encourage chemotaxis and biofilm formation by means we have not considered here (Sule et al, 2017; Meirieu et al., 1986).

It was hoped that the relationships would be laid bare as to direct attention for future designs by removing complication of large living systems, such as in mice. The author of this manuscript knows that application may be difficult as of yet, but as more variables are described, such testing becomes more reasonable and feasible. With the limitations of the molecules and the knowledge of other external factors, together with the added knowledge of the one-on-one interactions between the neurotransmitters and *E. coli*, I believe future experimentation to explain these phenomena is more clearly within sight.

FUTURE PERSPECTIVE

Regarding PEA's Role as a Chemoattractant Agent for E. coli

Some new questions come to mind, such as the following: is it PEA that acts as a chemoattractant, or is a degradative byproduct of PEA functions as a chemoattractant, similarly to Norepinephrine and DHMA? Or Which MCPs bind to PEA/byproducts, and how strongly does this ligand bind to the receptor? Or Is this physiological response to PEA specific to *E. coli* species, or does is function as a chemoattractant to bacterial species with various other classes of MCPs? Further research must be conducted to distinguish the role of PEA takes in the bacterial chemotactic system and will perhaps be useful in novel therapeutic or research methods.

Since PEA is generally regarded as safe (GRAS) and is found as an ingredient in various FDA approved products, it may serve to mitigate worries about use as a supplement (FDA Substances Added to Food, accessed 2020). Other compounds known to be metabolic products of both host and microbial metabolism are currently being studied in a similar research project currently ongoing, including phenylacetic acetate (PAA), which is an oxidation product of PEA.

Future research into the applicability of PEA and similar molecules may develop beyond dietary supplementation. Testing into the ability of PEA into the chemotaxis of other organisms, including pathogens, may determine the efficacy as a potential therapy for bacterial infection. Whereas most similar neurotransmitter compounds are fairly toxic at low concentrations (Norepinephrine and Epinephrine show an LD_{50} intravenous in the realm of 550µg/kg and 150µg/kg respectively, for example), related compounds like PEA are GRAS, under normal use (Pubchem, accessed 2020). PEA is both seen in various food products, such as chocolate, and as a weight loss or mood supplement (Ziegleder et al., 1992).

CONCLUSION

The author of this manuscript finds that there is a demonstrable relationship between neurotransmitter compound concentration and the regulation of *flhD*, the formation of biofilm, and in chemotaxis in several of the molecules tested. In addition to bolstering earlier literature detailing these relationships, there is now new information regarding a homolog of those neurotransmitters of which the capacity for encouraging chemotaxis is a central discovery. With knowledge of the chemoattractant qualities of PEA, a path may now open toward testing it in the interest of the development of some useful tool, perhaps as an agent in the protection from and alleviation of acute colitis caused by EHEC and related *E. coli* species (and perhaps other proteobacteria). In addition to other proposed health benefits of this molecule, its relative safety and ease of storage may make it a more useful object for testing that the relatively dangerous neurotransmitters in pure form. The possibilities for this little molecule are great indeed, and it is hoped this addition to our knowledge of its uses in comparison with its cousins may make it too tantalizing to be excluded from future comparison with those better recognized molecules.

It is the author's opinion that this study builds a firm foundation for future studies and may lead to real benefits in the field of medicine. It is hoped that this and related PEA research will discern these benefits as a low-cost alternative to other therapeutic methods and may relieve as much pain as possible and may further reduce costs which tax both the public purse and limited healthcare services. As the goal of research may often be to establish new information regarding the nature of the world and its living components, it is hoped that this information may also have the added benefit of creating some utility for those with the patience to understand it.

REFERENCES

Aiba H, Nakasai F, Mizushima S, Mizuno T. 1989. Phosphorylation of a bacterial activator protein, OmpR, by a protein kinase, EnvZ, results in stimulation of its DNA-binding ability. J Biochem 106:5–7. doi:10.1093/oxfordjournals.jbchem.a122817.

Aizawa, S. L., C.S. Harwood, and R.J. Kadner. 2000. Signaling components in bacterial locomotion and sensory reception. *J. Bacteriol*. **182**. 1459 - 71

Bansal T, Englert D, Lee J, Hegde M, Wood TK, Jayaraman A. 2007. Differential effects of epinephrine, norepinephrine, and indole on Escherichia coli O157:H7 chemotaxis, colonization, and gene expression. Infect. Immun. 75:4597–4607. 10.1128/IAI.00630-07.

Barker, C. S., Prüss, B. M., & Matsumura, P. 2004. Increased motility of Escherichia coli by insertion sequence element integration into the regulatory region of the flhD operon. Journal of bacteriology, 186(22), 7529–7537. doi:10.1128/JB.186.22.7529-7537.2004

Barnich N, Carvalho FA, Glasser A-L, Darcha C, Jantscheff P, Allez M, Peeters H, Bommelaer G, Desreumaux P, Colombel J-F, Darfeuille-Michaud A. 2007. CEACAM6 acts as a receptor for adherent-invasive E. coli, supporting ileal mucosa colonization in Crohn disease. J. Clin. Invest. 117:1566–1574

Baron EJ, Miller JM, Weinstein MP, et al. A guide to utilization of the microbiology laboratory for diagnosis of infectious diseases: 2013 recommendations by the Infectious Diseases Society of America (IDSA) and the American Society for Microbiology (ASM)(a). *Clin Infect Dis*. 2013;57(4):e22-e121. doi:10.1093/cid/cit278

Bartlett, D. H., B. B. Frantz, and P. Matsumura. 1988. Flagellar transcriptional activators FlbB and FlaI: gene sequences and 5′ consensus sequences of operons under FlbB and FlaI control. J. Bacteriol. 170:1575-1581.

Baumler AJ, Sperandio V. .2016.Interactions between the microbiota and pathogenic bacteria in the gut. Nature. 535:85–93. 10.1038/nature18849

Bellono, N. W., Bayrer, J. R., Leitch, D. B., Castro, J., Zhang, C., O'Donnell, T. A., … Julius, D. 2017. Enterochromaffin Cells Are Gut Chemosensors that Couple to Sensory Neural Pathways. Cell, 170(1), 185–198.e16. doi:10.1016/j.cell.2017.05.034

Ghodsalavi B, Svenningsen NB, Hao X, et al. A novel baiting microcosm approach used to identify the bacterial community associated with Penicillium bilaii hyphae in soil. *PLoS One*. 2017;12(10):e0187116. Published 2017 Oct 27. doi:10.1371/journal.pone.0187116

Berg HC, Brown DA. 1972. Chemotaxis in Escherichia coli analysed by three-dimensional tracking. Nature 239:500–504. doi: 10.1038/239500a0

Berg HC. 2003. The rotary motor of bacterial flagella. Annu Rev Biochem 72:19–54. doi:10.1146/annurev.biochem.72.121801.161737.

Berry, R. M., and J.P. Armitage. 1999. The bacterial flagellar motor. *Adv. Microb. Physiol.* **41**:291 - 337

Bourret RB, Stock AM. .2002. Molecular information processing: lessons from bacterial chemotaxis. J. Biol. Chem.;277:9625–9628.

Bren A, Eisenbach M. 1998. The N terminus of the flagellar switch protein, FliM, is the binding domain for the chemotactic response regulator, CheY. J Mol Biol 278:507–514. doi:10.1006/jmbi.1998.1730.

Briegel A, Li X, Bilwes AM, Hughes KT, Jensen GJ, Crane BR. 2012. Bacterial chemoreceptor arrays are hexagonally packed trimers of receptor dimers networked by rings of kinase and coupling proteins. Proc Natl Acad Sci U S A 109:3766–3771. doi:10.1073/pnas.1115719109.

Cameron EA, Sperandio V. 2015. Frenemies: signaling and nutritional integration in pathogen-microbiota-host interactions. Cell Host Microbe 18:275–284. doi:10.1016/j.chom.2015.08.007.

Carter M.Q., Louie J.W., Feng D., Zhong W., Brandl M.T. 2016. Curli fimbriae are conditionally required in Escherichia coli O157: H7 for initial attachment and biofilm formation. Food Microbiol.;57:81–89. doi: 10.1016/j.fm.2016.01.006

Castilho, B. A., Olfson, P., & Casadaban, M. J. 1984. Plasmid insertion mutagenesis and lac gene fusion with mini-mu bacteriophage transposons. Journal of bacteriology, 158(2), 488–495.

Cervi AL, Lukewich MK, Lomax AE. 2014. Neural regulation of gastrointestinal inflammation: role of the sympathetic nervous system. Auton Neurosci 182:83–88. doi:10.1016/j.autneu.2013.12.003.

Chen, Y. F., & Helmann, J. D. 1992. Restoration of motility to an Escherichia coli fliA flagellar mutant by a Bacillus subtilis sigma factor. Proceedings of the National Academy of Sciences of the United States of America, 89(11), 5123–5127. doi:10.1073/pnas.89.11.5123

Chervitz SA, Falke JJ. 1996. Molecular mechanism of transmembrane signaling by the aspartate receptor: a model. Proc Natl Acad Sci U S A 93:2545–2550. doi:10.1073/pnas.93.6.2545.

Ciapponi, A., Lewin, S., Herrera, C. A., Opiyo, N., Pantoja, T., Paulsen, E., … Oxman, A. D. 2017. Delivery arrangements for health systems in low-income countries: an overview of systematic reviews. The Cochrane database of systematic reviews, 9(9), CD011083. doi:10.1002/14651858.CD011083.pub2

Clarke, M. B., Hughes, D. T., Zhu, C., Boedeker, E. C., & Sperandio, V. 2006. The QseC sensor kinase: a bacterial adrenergic receptor. Proceedings of the National Academy of Sciences of the United States of America, 103(27), 10420–10425. doi:10.1073/pnas.0604343103

Clemente JC, Ursell LK, Parfrey LW, Knight R. 2012. The impact of the gut microbiota on human health: an integrative view. Cell. 148:1258–70. 10.1016/j.cell.2012.01.035

Costerton JW, Lewandowski Z, Caldwell DE, Korber DR, Lappin-Scott HM. 1995. Microbial biofilms. Annu Rev Microbiol 49:711–745. doi:10.1146/annurev.mi.49.100195.003431.
Costerton JW .1995. Overview of microbial biofilms. J Ind Microbiol 15: 137–140
Croxen, M. A., Law, R. J., Scholz, R., Keeney, K. M., Wlodarska, M., & Finlay, B. B. 2013. Recent advances in understanding enteric pathogenic Escherichia coli. Clinical microbiology reviews, 26(4), 822–880. doi:10.1128/CMR.00022-13

Dufour, Y. S., Gillet, S., Frankel, N. W., Weibel, D. B., & Emonet, T. 2016. Direct Correlation between Motile Behavior and Protein Abundance in Single Cells. PLoS computational biology, 12(9), e1005041. doi:10.1371/journal.pcbi.1005041

E. coli (Escherichia coli). (2019, November 22). Retrieved from https://www.cdc.gov/ecoli/index.html.
E. coli Genetic Resources at Yale CGSC, The Coli Genetic Stock Center. (n.d.). Retrieved from https://cgsc2.biology.yale.edu/.

Epinephrine. (2020, February 25). Retrieved from https://pubchem.ncbi.nlm.nih.gov/compound/5816 https://pubchem.ncbi.nlm.nih.gov/compound/439260

EVANS, D. G., MILES, A. A., & NIVEN, J. S. 1948. The enhancement of bacterial infections by adrenaline. *British journal of experimental pathology*, *29*(1), 20–39.

Falke, J. J., & Hazelbauer, G. L. 2001. Transmembrane signaling in bacterial chemoreceptors. *Trends in biochemical sciences*, *26*(4), 257–265. doi:10.1016/s0968-0004(00)01770-9

Fitzgerald, D. M., Bonocora, R. P., & Wade, J. T. 2014. Comprehensive mapping of the Escherichia coli flagellar regulatory network. PLoS genetics, 10(10), e1004649. doi:10.1371/journal.pgen.1004649

Fitzgerald, D. M., Smith, C., Lapierre, P., & Wade, J. T. 2018. The evolutionary impact of intragenic FliA promoters in proteobacteria. Molecular microbiology, 108(4), 361–378. doi:10.1111/mmi.13941

Foodborne Illnesses and Germs. (2019, October 23). Retrieved from https://www.cdc.gov/foodsafety/foodborne-germs.html.
Forst S, Delgado J, Inouye M. 1989. Phosphorylation of OmpR by the osmosensor EnvZ modulates expression of the ompF and ompC genes in Escherichia coli. Proc Natl Acad Sci U S A 86:6052–6056. doi:10.1073/pnas.86.16.6052.

Francez-Charlot A, Laugel B, Van Gemert A, Dubarry N, Wiorowski F, Castanie-Cornet MP, Gutierrez C, Cam K. 2003. RcsCDB His-Asp phosphorelay system negatively regulates the flhDC operon in Escherichia coli. Mol Microbiol 49:823–832. doi:10.1046/j.1365-2958.2003.03601.x.

Frankel, N. W., Pontius, W., Dufour, Y. S., Long, J., Hernandez-Nunez, L., & Emonet, T. 2014. Adaptability of non-genetic diversity in bacterial chemotaxis. eLife, 3, e03526. doi:10.7554/eLife.03526

Franzo, G., He, W., Correa-Fiz, F., Li, G., Legnardi, M., Su, S., & Segalés, J. 2019. A Shift in Porcine Circovirus 3 (PCV-3) History Paradigm: Phylodynamic Analyses Reveal an

Ancient Origin and Prolonged Undetected Circulation in the Worldwide Swine Population. Advanced science (Weinheim, Baden-Wurttemberg, Germany), 6(22), 1901004. doi:10.1002/advs.201901004

Furness JB, Rivera LR, Cho HJ, Bravo DM, Callaghan B. 2013. The gut as a sensory organ. Nat Rev Gastro Hepat. 10:729–740.

Girón, J. A., A. G. Torres, E. Freer, and J. B. Kaper. 2002. The flagella of enteropathogenic Escherichia coli mediate adherence to epithelial cells. Mol. Microbiol. 44:361-379.

González Barrios, A. F., R. Zuo, Y. Hashimoto, L. Yang, W. E. Bentley, and T. K. Wood. 2006. Autoinducer 2 controls biofilm formation in Escherichia coli through a novel motility quorum-sensing regulator (MqsR, B3022). J. Bacteriol. 188:305-316

Gottesman S., Stout V. 1991. Regulation of capsular polysaccharide synthesis in Escherichia coli K12. Mol. Microbiol. 5, 1599–1606. 10.1111/j.1365-2958.1991.tb01906.x

Gottesman, S., Trisler, P., & Torres-Cabassa, A. 1985. Regulation of capsular polysaccharide synthesis in Escherichia coli K-12: characterization of three regulatory genes. Journal of bacteriology, 162(3), 1111–1119.

Green BT, Brown DR. 2010. Interactions between bacteria and the gut mucosa. Do enteric neurotransmitters acting on the gut mucosal epithelium influence intestinal colonization or infection?, p 89–110 In Lyte ML, Freestone PPE, editors. (ed), Microbial endrocrinology: interkingdom signaling in infectious disease and health. Springer, New York, NY.

Hansen MC, Palmer RJ Jr, Udsen C, White DC, Molin S. 2001. Assessment of GFP fluorescence in cells of Streptococcus gordonii under conditions of low pH and low oxygen concentration. Microbiology 147:1383–1391. doi:10.1099/00221287-147-5-1383.

Hasan, R., Schaner, K., Schroeder, M., Wohlers, A., Shreffler, J., Schaper, C., Subramanian, H., & Brooks, A. 2019. Extended Release Combination Antibiotic Therapy from a Bone Void Filling Putty for Treatment of Osteomyelitis. *Pharmaceutics*, *11*(11), 592. https://doi.org/10.3390/pharmaceutics11110592

Hazelbauer GL, Falke JJ, Parkinson JS. 2008. Bacterial chemoreceptors: high-performance signaling in networked arrays. Trends Biochem. Sci. 33:9–19. 10.1016/j.tibs.2007.09.014.

Herrera Seitz MK, Soto D, Studdert CA. 2012. A chemoreceptor from Pseudomonas putida forms active signalling complexes in Escherichia coli. Microbiology 158:2283–2292. doi:10.1099/mic.0.059899-0.

Hoffmann S, Maculloch B, Batz M. 2015. Economic Burden of Major Foodborne Illnesses Acquired in the United States. United States Department of Agriculture. Available online at: https://www.ers.usda.gov/webdocs/publications/43984/52807_eib140.pdf

Horne SM, Schroeder M, Murphy J, Prüβ BM. 2018. Acetoacetate and ethyl acetoacetate as novel inhibitors of bacterial biofilm. Lett Appl Microbiol. 66:329–339

Horne, S. M., Sayler, J., Scarberry, N., Schroeder, M., Lynnes, T., & Prüß, B. M. 2016. Spontaneous mutations in the flhD operon generate motility heterogeneity in Escherichia coli biofilm. BMC microbiology, 16(1), 262. doi:10.1186/s12866-016-0878-1

Horner-Devine, M. C., M. Lage, J. B. Hughes, and B. J. M. Bohannan. 2004. A taxa-area relationship for bacteria. Nature 432:750-753.

Huerta AM, Collado-Vides J. 2003. Sigma70 Promoters in Escherichia coli: Specific Transcription in Dense Regions of Overlapping Promoter-like Signals. J Mol Biol 333: 261–278 10.1016/j.jmb.2003.07.017

Hughes, D. T., & Sperandio, V. 2008. Inter-kingdom signalling: communication between bacteria and their hosts. Nature reviews. Microbiology, 6(2), 111–120. doi:10.1038/nrmicro1836

Hughes, D. T., & Sperandio, V. 2008. Inter-kingdom signalling: communication between bacteria and their hosts. Nature reviews. Microbiology, 6(2), 111–120. doi:10.1038/nrmicro1836

Igo MM, Ninfa AJ, Stock JB, Silhavy TJ. 1989. Phosphorylation and dephosphorylation of a bacterial transcriptional activator by a transmembrane receptor. Genes Dev. 1989;3:1725–1734.

Irsfeld, M., Spadafore, M., & Prüß, B. M. (2013). β-phenylethylamine, a small molecule with a large impact. *WebmedCentral*, *4*(9), 4409.

Ishida K, Murata M, Katagiri N, Ishikawa M, Abe K, Kato M, Utsunomiya I, Taguchi K. 2005. Effects of beta-phenylethylamine on dopaminergic neurons of the ventral tegmental area in the rat: a combined electrophysiological and microdialysis study. J Pharmacol Exp Ther. 314(2):916–922.

Kaper, J. B., Nataro, J. P. & Mobley, H. L. 2004. Pathogenic Escherichia coli. Nat Rev Microbiol 2, 123–140, https://doi.org/10.1038/nrmicro818

Karavolos MH, Winzer K, Williams P, Khan CMA. 2013. Pathogen espionage: multiple bacterial adrenergic sensors eavesdrop on host communication systems. Mol. Microbiol. 87:455–465. 10.1111/mmi.12110.

Kawashima T. 2005. The autonomic nervous system of the human heart with special reference to its origin, course, and peripheral distribution. Anat Embryol (Berl) 209(6):425–438. doi: 10.1007/s00429-005-0462-1.

Kentner D, Sourjik V. 2006. Spatial organization of the bacterial chemotaxis system. Curr. Opin. Microbiol. 9:619–624

Kirby WM. 1944. Extraction of a highly potent penicillin inactivator from penicillin resistant staphylococci. Science 99:452–453. doi:10.1126/science.99.2579.452.

Kumari, S., Beatty, C. M., Browning, D. F., Busby, S. J., Simel, E. J., Hovel-Miner, G., & Wolfe, A. J. 2000. Regulation of acetyl coenzyme A synthetase in Escherichia coli. Journal of bacteriology, 182(15), 4173–4179. doi:10.1128/jb.182.15.4173-4179.2000

Kuroki T, Tsutsumi T, Hirano M, Matsumoto T, Tatebayashi Y, Nishiyama K, Uchimura H, Shiraishi A, Nakahara T, Nakamura K. 1990. Behavioral sensitization to beta-phenylethylamine (PEA): enduring modifications of specific dopaminergic neuron systems in the rat. Psychopharmacology (Berl) 102(5):10.

Kutsukake K, Iino T. 1994. Role of the FliA-FlgM regulatory system on the transcriptional control of the flagellar regulon and flagellar formation in Salmonella typhimurium. J Bacteriol 176:3598–3605.

Lindsay D, Brözel VS, Mostert JF, von Holy A. 2002. Differential efficacy of chlorine dioxide against single species and binary biofilms of a dairy-associated Bacillus cereus and a Pseudomonas fluorescens isolate. J. Appl. Microbiol. 92:352–361

Liu, X., & Matsumura, P. 1994. The FlhD/FlhC complex, a transcriptional activator of the Escherichia coli flagellar class II operons. Journal of bacteriology, 176(23), 7345–7351. doi:10.1128/jb.176.23.7345-7351.1994

Lomax AE, Sharkey KA, Furness JB. 2010. The participation of the sympathetic innervation of the gastrointestinal tract in disease states. Neurogastroenterol Motil. 22:7–18. 10.1111/j.1365-2982.2009.01381.x

Lynnes T, Horne SM, Prüß BM. 2014. ß-Phenylethylamine as a novel nutrient treatment to reduce bacterial contamination due to Escherichia coli O157:H7 on beef meat. Meat Sci 96:165–171

Zschiedrich CP, Keidel V, Szurmant H. 2016. Molecular mechanisms of two-component signal transduction. J Mol Biol 428:3752–3775. doi:10.1016/j.jmb.2016.08.003

Lyte M, Arulanandam BP, Frank CD. 1996. Production of Shiga-like toxins by Escherichia coli O157: H7 can be influenced by the neuroendocrine hormone norepinephrine. J Lab Clin Med 128:392–398. doi:10.1016/S0022-2143(96)80011-4.

Lyte M, Ernst S. 1992. Catecholamine induced growth of gram negative bacteria. Life Sci. 50:203–212. 10.1016/0024-3205(92)90273-R.

Macnab RM. 2003. How bacteria assemble flagella. Annu Rev Microbiol 57:77–100. doi:10.1146/annurev.micro.57.030502.090832.

Malakooti, J., Komeda, Y., & Matsumura, P. 1989. DNA sequence analysis, gene product identification, and localization of flagellar motor components of Escherichia coli. Journal of bacteriology, 171(5), 2728–2734. doi:10.1128/jb.171.5.2728-2734.1989

Mao H, Kremer PS, Manson MD. 2003. A senstive, versatile microfluidic assay for bacterial chemotaxis. Proc Natl Acad Sci U S A 100:5449–5454. doi:10.1073/pnas.0931258100.

Matilla MA, Krell T. 2017. Chemoreceptor-based signal sensing. Curr Opin Biotechnol 45:8–14. doi:10.1016/j.copbio.2016.11.021

Meirieu O, Pairet M, Sutra JF, Ruckebusch M. 1986. Local release of monoamines in the gastrointestinal tract: an in vivo study in rabbits. Life Sci 38:827–834. doi:10.1016/0024-3205(86)90599-0.

Mercuri NB, Saiardi A, Bonci A, Picetti R, Calabresi P, Bernardi G, Borrelli E. 1997. Loss of autoreceptor function in dopaminergic neurons from dopamine D2 receptor deficient mice. Neuroscience. 79(2):323–327.

Milligan DL, Koshland DE., Jr. 1988. Site-directed cross-linking. Establishing the dimeric structure of the aspartate receptor of bacterial chemotaxis. J Biol Chem. 1988;263(13):6268–6275

Moreira CG, Sperandio V. 2010. The epinephrine/norepinephrine/autoinducer-3 interkingdom signaling system of Escherichia coli O157:H7, p 213–227 In Lyte ML, Freestone PPE, editors. (ed), Microbial endrocrinology: interkingdom signaling in infectious disease and health. Springer, New York, NY.

Norepinephrine. (2020, February 25). Retrieved from https://pubchem.ncbi.nlm.nih.gov/compound/439260

Parales RE, Luu RA, Hughes JG, Ditty JL. 2015. Bacterial chemotaxis to xenobiotic chemicals and naturally occurring analogs. Curr Opin Biotechnol 33:318–326. doi:10.1016/j.copbio.2015.03.017.

Parkinson J. S. 1978. Complementation analysis and deletion mapping of Escherichia coli mutants defective in chemotaxis. Journal of bacteriology, 135(1), 45–53.

Parkinson JS, Parker SR. 1979. Interaction of the cheC and cheZ gene products is required for chemotactic behavior in Escherichia coli. Proc Natl Acad Sci USA. 76:2390–2394.

Pasupuleti, S., Sule, N., Manson, M. D., & Jayaraman, A. 2017. Conversion of Norepinephrine to 3,4-Dihdroxymandelic Acid in Escherichia coli Requires the QseBC Quorum-Sensing System and the FeaR Transcription Factor. Journal of bacteriology, 200(1), e00564-17. doi:10.1128/JB.00564-17

Phillips A, Navabpour S, Hicks S, Dougan G, Wallis T, Frankel G. 2000. Enterohaemorrhagic Escherichia coli O157:H7 target Peyer's patches in humans and cause attaching/effacing lesions in both human and bovine intestine. Gut 47:377–381. doi:10.1136/gut.47.3.377.

Proceedings of the National Academy of Sciences of the United States of America, 96(4), 1639–1644. doi:10.1073/pnas.96.4.1639

Prüß B. M. 2017. Involvement of Two-Component Signaling on Bacterial Motility and Biofilm Development. Journal of bacteriology, 199(18), e00259-17. doi:10.1128/JB.00259-17

Prüβ, B. M., J. W. Campbell, T. K. Van Dyk, C. Zhu, Y. Kogan, and P. Matsumura. 2003. FlhD/FlhC is a regulator of anaerobic respiration and the Entner-Doudoroff pathway through induction of the methyl-accepting chemotaxis protein Aer. J. Bacteriol. 185:534-543

Prüβ, B. M., Liu, J., Higgs, P. I., & Thompson, L. K. 2015. Lessons in Fundamental Mechanisms and Diverse Adaptations from the 2015 Bacterial Locomotion and Signal Transduction Meeting. Journal of bacteriology, 197(19), 3028–3040. doi:10.1128/JB.00384-15

Qin J, Li R, Raes J, Arumugam M, Burgdorf KSS, Manichanh C, et al. 2010. A human gut microbial gene catalogue established by metagenomic sequencing. Nature. 464:59–65. 10.1038/nature08821

Ramette, A., and J. M. Tiedje. 2007. Biogeography: an emerging cornerstone for understanding prokaryotic diversity, ecology, and evolution. Microb. Ecol. 53:197-207.

Rasamiravaka T, Labtani Q, Duez P, El Jaziri M. 2015. The formation of biofilms by Pseudomonas aeruginosa: a review of the natural and synthetic compounds interfering with control mechanisms. Biomed Res Int 2015:1–17

Rasko, D. A., Moreira, C. G., Li, d., Reading, N. C., Ritchie, J. M., Waldor, M. K., Williams, N., Taussig, R., Wei, S., Roth, M., Hughes, D. T., Huntley, J. F., Fina, M. W., Falck, J. R., & Sperandio, V. 2008. Targeting QseC signaling and virulence for antibiotic development. *Science (New York, N.Y.)*, *321*(5892), 1078–1080. https://doi.org/10.1126/science.1160354

Reboldi, A., & Cyster, J. G. 2016. Peyer's patches: organizing B-cell responses at the intestinal frontier. Immunological reviews, 271(1), 230–245. doi:10.1111/imr.12400

Römling, U., Galperin, M. Y., & Gomelsky, M. 2013. Cyclic di-GMP: the first 25 years of a universal bacterial second messenger. Microbiology and molecular biology reviews : MMBR, 77(1), 1–52. doi:10.1128/MMBR.00043-12

Roggo, C., Carraro, N., & van der Meer, J. R. 2019. Probing chemotaxis activity in Escherichia coli using fluorescent protein fusions. *Scientific reports*, *9*(1), 3845. doi:10.1038/s41598-019-40655-x

Ryan CA, Tauxe RV, Hosek GW, et al. 1986. Escherichia coli O157:H7 diarrhea in a nursing home: clinical, epidemiological, and pathological findings. J Infect Dis. 154:631–8.

Sabrina Pankey, M., Foxall, R. L., Ster, I. M., Perry, L. A., Schuster, B. M., Donner, R. A., … Whistler, C. A. 2017. Host-selected mutations converging on a global regulator drive an adaptive leap towards symbiosis in bacteria. eLife, 6, e24414. doi:10.7554/eLife.24414

Samanta, P., Clark, E. R., Knutson, K., Horne, S. M., & Prüß, B. M. 2013. OmpR and RcsB abolish temporal and spatial changes in expression of flhD in Escherichia coli biofilm. BMC microbiology, 13, 182. doi:10.1186/1471-2180-13-182

Segall JE, et al. 1986. Temporal comparisons in bacterial chemotaxis. Proc. Natl. Acad. Sci. U. S. A. 83:8987–8991.

Sourjik, V., & Wingreen, N. S. 2012. Responding to chemical gradients: bacterial chemotaxis. *Current opinion in cell biology*, *24*(2), 262–268.

Sowa Y, Berry RM. 2008. Bacterial flagellar motor. Q Rev Biophys 41:103–132.

Sperandio V, Torres AG, Kaper JB. 2002. Quorum sensing Escherichia coli regulators B and C (QseBC): a novel two-component regulatory system involved in the regulation of flagella and motility by quorum sensing in E. coli. Mol Microbiol 43:809–821. doi:10.1046/j.1365-2958.2002.02803.x.

Sperandio, V., Torres, A. G., Girón, J. A., & Kaper, J. B. 2001. Quorum sensing is a global regulatory mechanism in enterohemorrhagic Escherichia coli O157:H7. Journal of bacteriology, 183(17), 5187–5197. doi:10.1128/jb.183.17.5187-5197.2001

Sperandio, V., Torres, A. G., Jarvis, B., Nataro, J. P., & Kaper, J. B. 2003. Bacteria-host communication: the language of hormones. Proceedings of the National Academy of Sciences of the United States of America, 100(15), 8951–8956. doi:10.1073/pnas.1537100100

Substances Added to Food (Formerly EAFUS). 25. February 2020. Retrieved from https://www.accessdata.fda.gov/scripts/fdcc/?set=FoodSubstances&id=PHENETHYLAMINE

Sudo N. 2019. Biogenic Amines: Signals Between Commensal Microbiota and Gut Physiology. Frontiers in endocrinology, 10, 504. doi:10.3389/fendo.2019.00504

Sule, N., Pasupuleti, S., Kohli, N., Menon, R., Dangott, L. J., Manson, M. D., & Jayaraman, A. 2017. The Norepinephrine Metabolite 3,4-Dihydroxymandelic Acid Is Produced by the Commensal Microbiota and Promotes Chemotaxis and Virulence Gene Expression in Enterohemorrhagic Escherichia coli. Infection and immunity, 85(10), e00431-17. doi:10.1128/IAI.00431-17

Sule, P., Wadhawan, T., Carr, N. J., Horne, S. M., Wolfe, A. J., & Prüss, B. M. 2009. A combination of assays reveals biomass differences in biofilms formed by Escherichia coli mutants. Letters in applied microbiology, 49(3), 299–304. doi:10.1111/j.1472-765X.2009.02659.x

Surette MG, Levit M, Liu Y, Lukat G, Ninfa EG, Ninfa A, Stock JB. 1996. Dimerization is required for the activity of the protein histidine kinase CheA that mediates signal transduction in bacterial chemotaxis. J Biol Chem. 1996;271:939.

Surette, M. G., Miller, M. B., & Bassler, B. L. 1999. Quorum sensing in Escherichia coli, Salmonella typhimurium, and Vibrio harveyi: a new family of genes responsible for autoinducer production.

Szurmant H, Ordal GW. 2004. Diversity in chemotaxis mechanisms among the bacteria and archaea. Microbiol Mol Biol Rev 68:301–319. doi:10.1128/MMBR.68.2.301-319.2004.

Takeda S, Fujisawa Y, Matsubara M, Aiba H, Mizuno T. 2001. A novel feature of the multistep phosphorelay in Escherichia coli: a revised model of the RcsC → YojN → RcsB signalling pathway implicated in capsular synthesis and swarming behaviour. Mol Microbiol 40:440–450. doi:10.1046/j.1365-2958.2001.02393.x.

Trisler, P., & Gottesman, S. 1984. lon transcriptional regulation of genes necessary for capsular polysaccharide synthesis in Escherichia coli K-12. Journal of bacteriology, 160(1), 184–191.

Van Houdt R, Michiels CW. 2005. Role of bacterial cell surface structures in Escherichia coli biofilm formation. Res Microbiol. 2005;156(5):626–633. doi: 10.1016/j.resmic.2005.02.005

Wang, J., Dong, Y., Zhou, T., Liu, X., Deng, Y., Wang, C., Lee, J., & Zhang, L. H. 2013. Pseudomonas aeruginosa cytotoxicity is attenuated at high cell density and associated with the accumulation of phenylacetic acid. *PloS one*, *8*(3), e60187. https://doi.org/10.1371/journal.pone.0060187

Wang L, Rothemund D, Curd H, Reeves PR. 2003. Species-wide variation in the Escherichia coli flagellin (H-antigen) gene. J. Bacteriol. 185:2936–2943

Wong, C. S., S. Jelacic, R. L. Habeeb, S. L. Watkins, and P. I. Tarr. 2000. The risk of the hemolytic-uremic syndrome after antibiotic treatment of Escherichia coli O157:H7 infections. N. Engl. J. Med.

Zeng J, Spiro S. 2013. Finely tuned regulation of the aromatic amine degradation pathway in Escherichia coli. J Bacteriol 195:5141–5150. doi:10.1128/JB.00837-13.

Zhao, T., Doyle, M. P., Shere, J., & Garber, L. 1995. Prevalence of enterohemorrhagic Escherichia coli O157:H7 in a survey of dairy herds. Applied and environmental microbiology, 61(4), 1290–1293.

Zhou J, Lloyd SA, Blair DF. 1998. Electrostatic interactions between rotor and stator in the bacterial flagellar motor. Proc Natl Acad Sci U S A 95:6436–6441. doi:10.1073/pnas.95.11.6436.

Ziegleder G, Stojacic E, Stumpf B. 1992. Occurrence of beta-phenylethylamine and its derivatives in cocoa and cocoa products. *Z Lebensm Unters Forsch*;195:235–238